POLITECNICO DI MILANO

FACOLTÀ DI INGEGNERIA CIVILE, AMBIENTALE E TERRITORIALE

CORSO DI LAUREA IN INGEGNERIA CIVILE - INDIRIZZO STRUTTURE

TESI DI LAUREA SPECIALISTICA

LIMIT STATE DOMAIN OF HIGH DAMPING RUBBER BEARINGS IN SEISMIC ISOLATED NUCLEAR POWER PLANTS

Relatori:

Prof. Federico Perotti

Correlatori:

Ing. Giorgio Bianchi

Ing. Davide Carlo Mantegazza

ALLIEVO

Anaelle Ravez matr. 752073

Indice

Introduction:

This work is framed into the research activity performed at Politecnico di Milano within the field of seismic isolation of NPP (Nuclear Power Plant) buildings. One of the most challenging objectives for advanced NPPs is to identify cost effective engineering solutions to increase the current level of safety. Literature presents many factors affecting NPPs safety, among which an important role is played by the plant protection against external events, naturally or man-induced. The significant number of investigations recently performed worldwide has shown that earthquakes are among the most impacting external events in defining the annual damage frequency of nuclear reactor core. Moreover, it has been noticed that the risk induced by seismic events can be considered comparable with the risk caused by internally initiated events, because of the specific attitude of earthquakes to initiate multiple failure events. In the framework of a seismic Probabilistic Safety Assessment (PSA), fragility evaluation of safety related components is, therefore, a fundamental issue for a correct evaluation of risk. The seismic fragilities of single equipments shall be combined with the seismic hazard, i.e. the frequency of occurrence of a given intensity of the earthquake motion, to evaluate the probability of different core damage states.

The NPPs are designed for Serviceability Limit State (SLS) earthquake and for Ultimate Limit State (ULS) earthquake. The first is of medium intensity with higher return probability, after which the plant shall be operative with minor maintenance. The latter is of higher intensity with a lower return probability, after which a huge crisis shall be prevented by keeping all radioactive components contained and cooled.

Recent seismic events in Japan induced significant damages to NPPs (July 2007 - Kashiwakazi NPP; March 2011 – Fukushima NPP) and focused world public opinion on the risk due to major earthquakes. In particular, Fukushima NPP, put into operation in the 70's-80's, suffered accelerations widely bigger than designed at the time (the registered acceleration were between 3,3 and 6,4 m/s^2; design ones were between 2,4 and 3,2 m/s^2).

Recent studies performed at Politecnico the Milano (2006-2011) adopted the IRIS reactor (International Reactor Innovative and Secure) as reference case to develop innovative solutions in reducing the seismic hazard. IRIS is an integral, modular, medium size (335MWe) Pressurized Water Reactor (PWR), whose preliminary design was developed through an international partnership including over twenty organizations from nine countries, which provides a viable bridge to Generation IV reactors. Its features include safety equipments which can be activated without human intervention or electricity, also known as passive systems, and base isolation system at foundation level.

Results of these studies identified base isolation system as one of the most effective technical solution to mitigate seismic risk. In particular:

- Isolation system leads to much lower horizontal peak accelerations. The frequency energy content of the absolute accelerations at different locations is significant only in low frequency range (0.3÷2 Hz), and common NPPs components usually exhibit natural frequencies higher than 5÷10 Hz.

- The Soil-Structure Interaction (SSI) becomes less important for horizontal vibration modes. Safety assessments and design procedures become less dependent on the actual soil dynamic stiffness and damping.
- Horizontal accelerations are almost the same throughout the building. This facilitates the design of safety related components, since the seismic demand is the same regardless of the floor level, allowing a simpler and less conservative design, which leads to more standardized equipments.
- the main contributor to seismic risk becomes the isolation system itself. Reliable limit state domains shall be defined both for first-damage and complete failure conditions, in order to perform PSA.

In previous works published by Politecnico di Milano, a complete FE HDRB model, consisting of alternate high damping rubber and steel layers, was set and extensive numerical tests were performed to identify the most suitable element type, mesh refinement and analysis parameters, in order to account for highly nonlinear geometric and mechanical material properties. At the same time, a refined FE model of a single rubber layer was developed to investigate in detail different ANSYS® hyperelastic material models and tune them against experimental results.

In the present study, the development of a new FE model of a HDRB in ANSYS® has been pursued, mainly aimed at the definition of a reliable limit state domain under seismic excitation. Along with the numerical domain, an analytical approach was developed to support designers with a computational efficient tool. A theoretical framework of mechanical continuum is firstly given and, after a comprehensive study of the global and local behavior of numerical and analytical models, a limit state domain for delamination mode is assessed in terms of both stresses and global actions. Finally, the influence of the compressibility on stresses and on limit state domains is approached.

I. Seismic protection of Nuclear Power Plants:

A. Seismic design:

In the NPP of the new generation like IRIS the probability of internal failure has been drastically reduced of 2 to 3 orders of magnitude, thus the external risks have become the determinant one. The seism is one important external risk and has to be studied precisely.

The seismic isolation considerably increases the performance the building in terms of acceleration response to design seismic actions. To ensure this they are themselves put through great displacements. The isolator can therefore become the critical components.

Seismic design of traditional and isolated buildings will be presented in the following part. The traditional building will be considered linear while for the isolated one mechanical non linearity will be taken into account. The seismic risk will be defined as the combination of the structure fragility and the hazard of the site. Then the calculus of the vulnerability through the response surface methodology and the Monte Carlo simulation will be detailed. For the isolated building once the new risk variable defined, the response surface is calculated through the failure domain.

1. Seismic risk:

The following variable will be used in the definition of the seismic risk:

$$DM = Damage\ Measure;\ limit\ value\ dmf$$
$$EDP = Engineering\ Demand\ Paramater$$
$$IM = Intensity\ Measure$$

The EDP is the dynamic excitation (acceleration, displacement…) due to the global response and imposed to the **structure**.

The IM (Peak Ground Acceleration, spectral acceleration …) give the severity of earthquake motion on the NPP **site**.

According to the Pacific Earthquake Engineering Research (PEER), the seismic risk can be expressed as:

$$P_f = \iint P(DM > dmf|EDP = edp)p_{EDP}(edp|IM = im)p_{IM}(im)d(edp)d(im)$$

In a first approach, the damage analysis step is avoided and the risk can directly be expressed through EDP:

$$P_f = \int P_{EDP}(EDP > edpf|IM = im)p_{IM}(im)d(im)$$

The seismic risk is the convolution product between structure vulnerability and site hazard. The fragility function is defined as:

$$F(edp, im) = P(EDP > edp|IM = im) = 1 - P_{EDP}(edp/IM = im)$$

$$P_{EDP}(edp\ /IM = im):\ conditional\ core\ damage\ frequency\ for\ edp\ variable$$

2. Fragility analysis:

a) Traditional building:

First the EDP and the IM taken into consideration need to be defined. The fragility function will be expressed in function of its associated limit state function. This limit state function depends on a response. In this case this response will be expressed trough finite element simulation; the fitted values are the mean and the standard deviation. Once the response and thus the limit state function determined the fragility will be calculated integrating the density of probability with Monte Carlo Simulation. The fragility curve will be plotted calculating the fragility for different peak amplification.

For a non isolated building, the maximum value *A* of the acceleration at the component supports should be considered as EDP; the most severe peak ground horizontal acceleration A_g defined *IM*.

The traditional non isolated building is considered linear (as all the non linearity can be treated in the damage analysis). In this case the fragility function can be seen as the probability to exceed a noted dynamic amplification:

$$F(edp, im) = P\{A > a|A_g = a_g\} = P_{exc}(a, a_g) = P_{exc}(a/a_g)$$

If the seismic input is stochastic the probability to exceed a value is associated to a limit state function:

$$g(X, a, a_g) = C - D(X, a_g) = a - R(X)a_g = 0$$

$$g: performance\ function$$

$$X: vector\ of\ the\ random\ variables$$

$$R: response\ to\ a\ unit\ peak\ ground\ acceleration$$

The expression can be written taking the peak amplification factor $\frac{a}{a_g}$ as EDP:

$$\tilde{g}\left(X, \frac{a}{a_g}\right) = \frac{a}{a_g} - R(X)$$

The fragility function thus becomes:

$$F(edp, im) = P(\tilde{g}(X) < 0) = \iint_{\tilde{g}<0} p_R(r, x) dr dx$$

Once the distributions of probability of X and the probability of exceeding limit state R have been chosen, the integral can be calculated by the method of Monte Carlo simulation.

R can be found through a structural dynamic analysis of a finite elements model for every realization of random variable X. For complex model as the number of iteration in the Monte Carlo method is consequent, the numerical cost can be high.

R is determined trough the response surface method. The response function is approximated by a function; the mean μ_R and the standard deviation σ_R are the fitted quantities.

In this case R is found with a simulation approach. With the spectral parameters appearing in X, the ground motion is simulated. For each random vibration problem the mean and the variance of R are estimated from the finite element model solution. This operation is repeated the needed number of time in order to determinate the parameter of μ_R andσ_R.

To compute the fragility curve the fragility function has to be calculated for different peak amplification (a/a_g) but the response function stays the same.

b) Isolated building:

To reduce accelerations in the building, the system is isolated with HDRB devices. To ensure this reduction these isolator are submitted to important horizontal displacement. The isolators are the critical elements: the failure of the system is closely linked to the failure of the isolator.

Therefore the choice of the EDP is changed; the significant value with respect to the failure is now the displacement of the most strained isolator. Thus the fragility function becomes:

$$F(edp, im) = P\left(U > u \middle| A_g = a_g\right) = P_{exc}\left(u, a_g\right)$$

The behavior of the isolator is non linear, indeed no linearization are used. For a fixed ag, the response surface could be determined as before, the integral can be computed with Monte Carlo method:

$$P_{exc}\left(u, a_g\right) = \iiint_{g<0} p(u, x) du dx$$

Nevertheless due to non linearity, to plot the failure curve the response surface will be different for every peak acceleration (ag). This potentially represents a really high numerical cost even if the structural model can be much simple.

The limit state function can otherwise be expressed in terms of horizontal and vertical loads applied on the most strained isolator. The definition of an accurate domain to define precisely the fragility curve is the scope of this study.

Once the domain defined we will be able to obtain the failure curve through the limit state function defined as:

$$g(X, ag) = 1 - \frac{SC(X, ag)}{SL(X, ag)} = 0$$

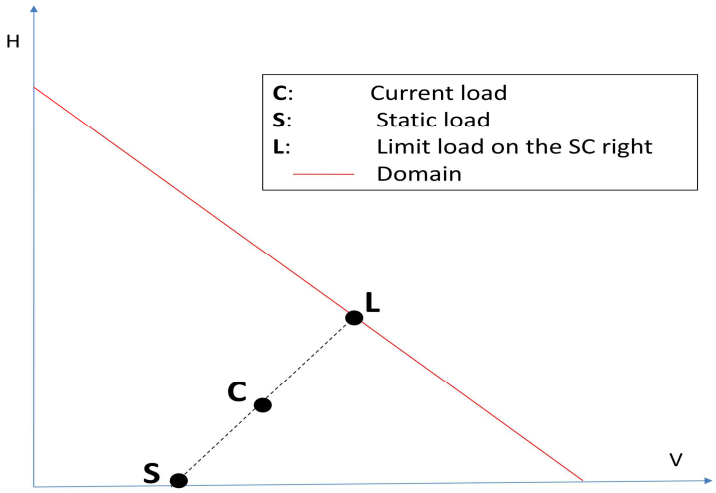

It has been shown the importance to have an accurate H/V domain for the isolator to obtain the failure curve which is an essential step to proceed with the seismic risk analysis.

B. High Damping Rubber Bearings (HDRB):

The device studied is a seismic isolator HDRB (High Damping Rubber Bearings) used in nuclear power plants made under IRIS program. It's made of alternative layer of rubber and steel as shown on the picture:

Figure 1: Picture of an isolator (not actual dimensions)

Its characteristics (geometry, materials, mechanic behavior...) are recapitulated in the following tables:

Isolator external diameter	**D**	**1000**	**mm**
Steel reinforcing plate diameter	D'	980	mm
Thickness of the internal steel plates	ts	4	mm
Number of elastomeric layers		10	
Thickness of one elastomeric layer	ti	10	mm
Total elastomeric thickness	Te	100	mm
First shape factor	S	24	
Second shape factor	S	9,6	
Dynamic shear modulus	**G**	**1,4**	**Mpa**

The mechanical characteristics of the isolator have been found for the scaled isolator 1/2, for accuracy reason they will be given for this scaled isolator:

Characteristics	Unit	Reference Code	Measured value	Requirement
Hardness	Shore A3	UNI EN ISO 868	72.5	75±3
Tensile strength	N/mm^2	UNI 6065	17.5	≥ 15.5
Elongation at break	%	UNI 6065	735	≥ 350
90° Peel method (Adhesion to metal)	N/mm	UNI 5405	19.0	≥ 350
Compression set (25% - 24 h - 70°C)	%	UNI 4913	19.1	≤ 20
Low temperature resistance	°C	UNI 7320	-60	≤ -25
Ozone resistance (20% - 90 h – 40°C)	see	UNI ISO 1431-1	no cracks	no cracks
Characteristics after air aging (168 h; 70°C)				
Δ hardness	ShA3'	UNI ISO 188	+5	±10
Δ tensile strength	N/mm^2	UNI ISO 188	-7	≥ -15
Δ elongation at break	%	UNI ISO 188	-17	≥ -20

Figure 2: mechanicals proprieties of the ½ scaled isolator

II. Basics of elasticity:

A. Basics of linear algebra:

The main mathematical object we are dealing with in continuum mechanics are the tensor, they are represented by matrix. In many cases those matrix are real and symmetric. In order not to repeat them every time, the main proprieties of those matrixes will be described in this paragraph.

1. Diagonal form:

Real symmetric matrixes have real eigenvalues and can be put in a diagonal form in an orthonormal basis.

For example if $\lambda_1,\ \lambda_2\ ,\ \lambda_3$ are the three eigenvalues of a real symmetric matrix of the third order $\bar{\bar{A}}$, and $n_1,\ n_2, n_3$ are the associated eigenvectors; $n_1,\ n_2, n_3$ can be chosen in order to form an orthonormal basis and:

$$\bar{\bar{A}} = \begin{bmatrix} n_1 & n_2 & n_3 \end{bmatrix} \begin{bmatrix} \lambda_1 & 0 & 0 \\ 0 & \lambda_2 & 0 \\ 0 & 0 & \lambda_3 \end{bmatrix} \begin{bmatrix} {n_1}^t \\ {n_2}^t \\ {n_3}^t \end{bmatrix}$$

2. Invariant of a matrix:

For a square matrix some quantities don't depend on the basis in which the matrix is expressed, these quantities are called invariant.

The determinant, the trace and the eigenvalues of a square matrix are invariants.

For the further developments we will define three invariants I1 I2 and I3, referring to the case of a square matrix 3*3, which is our usual situation. They correspond to the coefficient of the characteristic polynomial R(λ); the roots of this polynomial are the eigenvalues:

$$R(\lambda) = -\lambda^3 + I1\lambda^2 - \mathrm{I}2\lambda + I3$$

They have the following definition:

$$I1 = tr\left(\bar{\bar{A}}\right) = a_{11} + a_{22} + a_{33}$$
$$I2 = second\ minor\ of\ A = a_{11}a_{22} + a_{11}a_{33} + a_{33}a_{22} - a_{12}a_{21} - a_{13}a_{31} - a_{32}a_{23}$$
$$I3 = \det(\bar{\bar{A}})$$

They can be easily expressed in function of the eigenvalues:

$$I1 = \lambda_1 + \lambda_2 + \lambda_3$$
$$I2 = \lambda_1\lambda_2 + \lambda_2\lambda_3 + \lambda_3\lambda_1$$
$$I3 = \lambda_1\lambda_2\lambda_3$$

B. Continuum mechanics:

1. Cauchy's continuum:

We consider a continuum that occupies a volume **V** and is delimitated by a surface **S**. On this continuum are acting body loads and surface loads. The resultant of these actions on a finite part of the volume or the surface can be seen as the resultant of the forces **ΔR** applied on a point and the resultant of the moment **ΔM** with respect to this point**.**

The hypothesis of the Cauchy's continuum stipulates that:

$$\lim_{\Delta V \to 0} (\Delta \mathrm{R}/\Delta \mathrm{V}) = \mathrm{F}$$

$$\lim_{\Delta S \to 0} (\Delta \mathrm{R}/\Delta \mathrm{S}) = \mathrm{f}$$

$$\lim_{\Delta V \to 0} (\Delta \mathrm{M}/\Delta \mathrm{V}) = 0$$

$$\lim_{\Delta S \to 0} (\Delta \mathrm{M}/\Delta \mathrm{S}) = 0$$

Due to this hypothesis all the concentrated load should always considered distributed on a surface even really small.

2. Cauchy's stress tensor:

We now consider a Cauchy continuum in equilibrium. We make the hypothesis to divide this continuum ideally in two parts. For this continuum to remain in equilibrium actions should exchanged by the separation surface.

We consider a point P that stands on the separation surface of one of the piece of continuum, $\Delta\Sigma$ a finite area around P and the vector n_α the outgoing normal to the surface $\Delta\Sigma$.

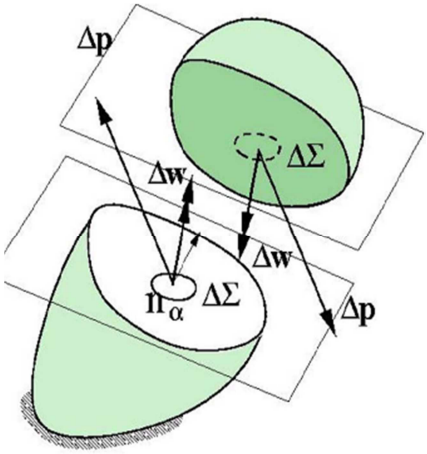

Figure 3: Cauchy continuum ideally split into two parts

We suppose that:

$$\lim_{\Delta S \to 0} (\Delta R/\Delta S) = \Delta p = \sigma_\alpha$$

$$\lim_{\Delta S \to 0} (\Delta M/\Delta S) = \Delta w = 0$$

σ_α is called stress and it has the following propriety:

$$\sigma_{-\alpha} = -\sigma_\alpha$$

The Cauchy stress is entirely determined if its components are known on an orthonormal basis:

$$\sigma_\alpha = \bar{\bar{\sigma}} n_\alpha$$

Where $\bar{\bar{\sigma}}$ is the Cauchy stress tensor which is symmetric and noted as:

$$\bar{\bar{\sigma}} = \begin{matrix} \sigma_{xx} & \tau_{xy} & \tau_{xz} \\ \tau_{xy} & \sigma_{yy} & \tau_{yz} \\ \tau_{xz} & \tau_{yz} & \sigma_{zz} \end{matrix}$$

These stresses can be seen on the following figure:

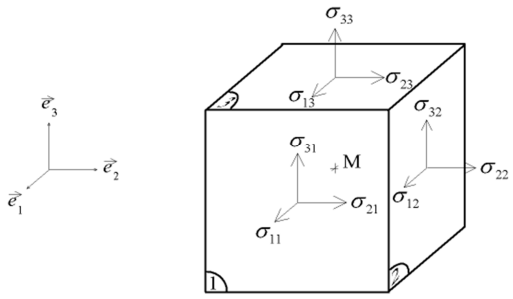

3. The different components of the deformation:

We consider an undeformed continuum Γ_0 at the time t_0 . We put it trough changes that gives it a different configuration Γ at the time t.

We choose a point P on this continuum, at the time t_0 its coordinates are X_0 whereas at the time t its position is given by x(X_0, t). The displacement of P between t_0 and t is given by the vector s.

$$x = X_0 + s$$

The **compatibility** hypothesis stipulates that the displacement occurs without superposition of material. For this to be verified the displacement should depend only on X_0 and should be a continuous function of this variable. Furthermore the displacement should verify the boundary conditions.

Let's consider two points P_0 and P on the continuum in the initial configuration, after the deformation they become p_0 and p. The velocity of P is done by the following relation as the initial position of P, X_0 does not depend on the time:

$$v(x,t) = \frac{dx}{dt} = \frac{ds}{dt}$$

We can express the velocity of p in function of the velocity of p_0 and of the relative velocity dv:

$$v(x,t) = v_0 + dv = v_0 + \frac{\partial v}{\partial x}dx = v_0 + \bar{\bar{L}}dx$$

The quantity $\bar{\bar{L}}$ can be defined from this relation. $\bar{\bar{L}}$ is a tensor and is called velocity gradient. $\bar{\bar{L}}$ can be decomposed in two parts: the symmetric part $\bar{\bar{D}}$ and the antisymmetric part $\bar{\bar{W}}$, then:

$$v(x,t) = v_0 + \bar{\bar{D}}dx + \bar{\bar{W}}dx$$

The velocity is now decomposed in three components: $\boldsymbol{v_0}$ the **rigid translation**, $\bar{\bar{\boldsymbol{W}}}$ the **rigid rotation** and $\bar{\bar{\boldsymbol{D}}}$ the **pure strain**. This last component is the one that interest us the most.

4. A measure of the pure deformation: Green-Lagrange tensor

A finite measure of strain will be introduced in the following paragraph. It can be introduced from two points of view: focusing on the initial configuration or on the current one. The first one is called Lagrangian approach the second one Eulerian approach. For our case the Lagragian approach has been chosen.

We look for a relationship between dx (the distance between p and p_0) and dX_0 (the distance between P and P_0):

$$dx = \bar{\bar{F}}dX_0 = \frac{\mathrm{dx}}{\mathrm{d}X_0} = \frac{\mathrm{d}(X_0 + s)}{\mathrm{d}X_0} = \bar{\bar{\mathrm{I}}} + \frac{\mathrm{ds}}{\mathrm{d}X_0}$$

$\bar{\bar{F}}$ is named strain gradient, it's a strain measure but not of pure deformation as it also include the deformation due to the rigid rotation. In order to separate the two contributions we calculate the square of the distance:

$$\mathrm{d}X_0^2 = \mathrm{d}X_0{}^{\mathrm{t}}\mathrm{d}X_0$$
$$dx^2 = dx^t dx = \mathrm{d}X_0{}^{\mathrm{t}}\bar{\bar{F}}^t\bar{\bar{F}}\mathrm{d}X_0$$
$$dx^2 - \mathrm{d}X_0^2 = \mathrm{d}X_0{}^{\mathrm{t}}\left(\bar{\bar{F}}^t\bar{\bar{F}} - \bar{\bar{\mathrm{I}}}\right)\mathrm{d}X_0 = 2\mathrm{d}X_0{}^{\mathrm{t}}\bar{\bar{E}}\mathrm{d}X_0$$

$\bar{\bar{E}}$ is the Green-Lagrange strain tensor and it's an actual measure of pure deformation. We can also define C the right Cauchy-Green tensor and B the left Cauchy-Green tensor:

$$\bar{\bar{C}} = \bar{\bar{F}}^t\bar{\bar{F}}$$
$$B = \bar{\bar{F}}\bar{\bar{F}}^t$$

5. The stress tensor associated with $\bar{\bar{E}}$: the Piola-Kirchhoff tensor

The velocity of deformation tensor $\bar{\bar{D}}$ is associated to the Cauchy stress tensor through the virtual work principle. $\frac{d\,\bar{\bar{E}}}{dt}$ is analogous to $\bar{\bar{D}}$. We define the Piola-Kirchhoff stress tensor $\bar{\bar{S}}$ as the associated quantity to $\frac{d\,\bar{\bar{E}}}{dt}$ trough the virtual work principle.

$$\int_V \sigma_{ij}(x)D_{ij}(x)dV = \int_{V_0} S_{ij}(X_0)\dot{E_{ij}}(X_0)dV_0$$

In order to determine a relation between $\bar{\bar{S}}$ and $\bar{\bar{\sigma}}$ we have to express $\frac{d\,\bar{\bar{E}}}{dt}$in function of $\bar{\bar{D}}$ and to define the transformation x=x(X_0).

To express the derivate of $\bar{\bar{E}}$ with respect of time with first have to determine $\frac{d\,\bar{\bar{F}}}{dt}$

$$\frac{d\,\bar{\bar{F}}}{dt} = \frac{d}{dt}\frac{\mathrm{dx}}{\mathrm{d}X_0} = \frac{dv}{dX_0} = \frac{dv}{dx}\frac{dx}{dX_0} = \bar{\bar{L}}\bar{\bar{F}}$$
$$\frac{d\,\bar{\bar{E}}}{dt} = \frac{1}{2}\frac{d}{dt}(\bar{\bar{F}}^t\bar{\bar{F}} - \bar{\bar{\mathrm{I}}}) = \frac{1}{2}\left(\frac{d\bar{\bar{F}}^{\bar{\bar{t}}}}{dt}\bar{\bar{F}} + \bar{\bar{F}}^t\frac{d\bar{\bar{F}}}{dt}\right) = \frac{1}{2}\bar{\bar{F}}^t(\bar{\bar{L}}^t + \bar{\bar{L}})\,\bar{\bar{F}} = \bar{\bar{F}}^t\bar{\bar{D}}\,\bar{\bar{F}}$$
$$\bar{\bar{D}} = \bar{\bar{F}}^{-t}\frac{d\,\bar{\bar{E}}}{dt}\,\bar{\bar{F}}^{-1}$$

The determinant of $\bar{\bar{F}}$ is the Jacobian of the transformation x=x(X_0):

$$J = \det(\bar{\bar{F}})$$

We can now transform the integral:

$$\int_V \sigma_{ij}(x) D_{ij}(x) dV = \int_V \sigma_{ij}(x) \frac{dX_h}{dx_i} \frac{dX_k}{dx_j} \dot{E_{hk}}(x) dV$$

$$\int_V \sigma_{ij}(x) \frac{dX_h}{dx_i} \frac{dX_k}{dx_j} \dot{E_{hk}}(x) dV = \int_{V_0} J\sigma_{ij} \frac{dX_h}{dx_i} \frac{dX_k}{dx_j} \dot{E_{hk}} dV_0 = \int_{V_0} S_{ij}(X_0) \dot{E_{\iota j}}(X_0) dV_0$$

We can deduce that:

$$\bar{\bar{S}} = J\bar{\bar{F}}^{-t} \bar{\bar{\sigma}}\, \bar{\bar{F}}^{-1}$$

$$\bar{\bar{\sigma}} = \frac{1}{J} \bar{\bar{F}}^{t} \bar{\bar{S}}\, \bar{\bar{F}}$$

6. Small displacement hypothesis: infinitesimal strain tensor

The two assumptions of the small displacement hypothesis are:

1. The displacements and the deformations are small enough to be able to assimilate the initial speed to the displacement.
2. The displacements and the deformations are small enough not to influence the way how this equilibrium is established. I.e. the equilibrium can be imposed in the initial configuration.

We can define the displacement gradient (analog to $\bar{\bar{F}}$) that will be noted $\bar{\bar{\psi}}$:

$$\bar{\bar{\psi}} = \frac{\mathrm{ds}}{\mathrm{dx}}$$

As before the pure deformation part of the displacement gradient is its symmetric part:

$$\bar{\bar{\varepsilon}} = \frac{1}{2}\left(\bar{\bar{\psi}} + \bar{\bar{\psi}}^{t}\right)$$

$$\bar{\bar{\varepsilon}} = \begin{bmatrix} \frac{\partial s_1}{\partial x_1} & \frac{1}{2}\left(\frac{\partial s_1}{\partial x_2} + \frac{\partial s_2}{\partial x_1}\right) & \frac{1}{2}\left(\frac{\partial s_1}{\partial x_3} + \frac{\partial s_3}{\partial x_1}\right) \\ \frac{1}{2}\left(\frac{\partial s_1}{\partial x_2} + \frac{\partial s_2}{\partial x_1}\right) & \frac{\partial s_2}{\partial x_2} & \frac{1}{2}\left(\frac{\partial s_2}{\partial x_3} + \frac{\partial s_3}{\partial x_2}\right) \\ \frac{1}{2}\left(\frac{\partial s_1}{\partial x_3} + \frac{\partial s_3}{\partial x_1}\right) & \frac{1}{2}\left(\frac{\partial s_2}{\partial x_3} + \frac{\partial s_3}{\partial x_2}\right) & \frac{\partial s_3}{\partial x_3} \end{bmatrix}$$

C. Constitutive law:

In the precedent part we have introduced stresses and strains in the case of finite deformation and small displacement theory. We now need to define a link between these two quantities. This link mainly depends on the material; the mathematical model created to describe this relation is called constitutive law.

1. Linear elasticity:

The existence of a deformation potential is assumed. This potential is named deformation energy and has the following expression:

$$\omega(\varepsilon) = \int_0^{\varepsilon_{ij}} \sigma_{ij} d\,\varepsilon_{ij}$$

The energy depends only on the final point and not on how it arrives on the final point. To verify this condition ω should an exact differential. Thus:

$$\frac{\partial \sigma_{ij}}{\partial \varepsilon_{kl}} = \frac{\partial \sigma_{kl}}{\partial \varepsilon_{ij}}$$

We have supposed an elastic linear constitutive law; therefore we can assume the existence of a tensor of the 4th order D_{ijkl}:

$$\sigma_{ij} = D_{ijkl}\varepsilon_{kl}$$

$$D_{ijkl} = \frac{\partial \sigma_{ij}}{\partial \varepsilon_{kl}}$$

The exact differential condition reduces the number of parameters. Furthermore the material is considered isotropic; the energy can therefore be express in function of the three deformation invariants. Combining all those conditions the constitutive law takes the following form:

$$\bar{\bar{\sigma}} = \begin{bmatrix} \lambda+2G & \lambda & \lambda & 0 & 0 & 0 \\ \lambda & \lambda+2G & \lambda & 0 & 0 & 0 \\ \lambda & \lambda & \lambda+2G & 0 & 0 & 0 \\ 0 & 0 & 0 & G & 0 & 0 \\ 0 & 0 & 0 & 0 & G & 0 \\ 0 & 0 & 0 & 0 & 0 & G \end{bmatrix} \bar{\bar{\varepsilon}}$$

$$E = G\frac{3\lambda + 2G}{\lambda + G}$$

$$\nu = \frac{\lambda}{2(\lambda + G)}$$

2. Hyperelasticity:

The material is considered hyperelastic or **elastic non linear**. Indeed the relation between strain and stress is not linear but the phenomenon is reversible and does not dissipate energy. The case **incompressible** material will be seen. The material will also be considered **isotropic**.

a) Finite deformation theory:

(1) Hyperelastic isotropic material:

In the previous paragraph the following quantities have been introduced:

$$\bar{\bar{\boldsymbol{\sigma}}} : Cauchy\ stress\ tensor$$

$$\bar{\bar{\boldsymbol{S}}} : Piola\ stress\ tensor$$

$$\boldsymbol{s} : Displacement\ vector$$

$$\bar{\bar{\boldsymbol{F}}} = \bar{\bar{I}} + \overline{\overline{grad}}(s)\ Strain\ tensor$$

$$\bar{\bar{\boldsymbol{B}}} = \bar{\bar{F}}\bar{\bar{F}}^t\ Left\ Cauchy/Green\ tensor$$

$$\bar{\bar{\boldsymbol{C}}} = \bar{\bar{F}}^t\bar{\bar{F}}\ Right\ Cauchy/Green\ tensor$$

$$\boldsymbol{J} = \det\left(\bar{\bar{F}}\right)\ Jacobiano$$

The following relation has been established:

$$\bar{\bar{\sigma}} = J^{-1}\bar{\bar{F}}\bar{\bar{S}}\bar{\bar{F}}^t$$

C and B are real symmetric matrix so they have tree real eigenvalues. They have the same invariant I1 I2 and I3:

$$I1 = C11 + C22 + C33$$

$$I2 = C11C22 + C11C33 + C22C33 - C12^2 - C13^2 - C23^2$$

$$I3 = \det(C)$$

Our material is **hyperelastic**, thus we can suppose the existence of a **strain energy function W**. For the rubber model several form of the strain energy functions have been tested and the more accurate has been chosen (POLY-2P). The generic equation of σ (express in function of W) will be presented first, and then the equation of the model chosen will be developed.

The derivative of W with respect to one of the strain tensor is the corresponding stress S:

$$2\frac{\partial W}{\partial \bar{\bar{C}}} = \bar{\bar{S}}$$

The second hypothesis is that the material is **isotropic**; therefore W only depends on the invariant I1 I2 I3.

$$W\left(\bar{\bar{C}}\right) = W(I1, I2, I3)$$

We differentiate W with respect to the invariant:

$$\frac{\partial W}{\partial \bar{\bar{C}}} = \frac{\partial W}{\partial I1}\frac{\partial I1}{\partial \bar{\bar{C}}} + \frac{\partial W}{\partial I2}\frac{\partial I2}{\partial \bar{\bar{C}}} + \frac{\partial W}{\partial I3}\frac{\partial I3}{\partial \bar{\bar{C}}}$$

$$\frac{\partial W}{\partial \bar{\bar{C}}} = \frac{\partial W}{\partial I1}\bar{\bar{I}} + \frac{\partial W}{\partial I2}\left(I1\bar{\bar{I}} - \bar{\bar{C}}\right) + \frac{\partial W}{\partial I3}I3\bar{\bar{C}}^{-1}$$

We know calculate the Cauchy stress:

$$\bar{\bar{\sigma}} = J^{-1}\bar{\bar{F}}\bar{\bar{S}}\bar{\bar{F}}^{t} = 2J^{-1}\left(\bar{\bar{F}}\bar{\bar{I}}\bar{\bar{F}}^{t}\left(\frac{\partial W}{\partial I1} + I1\frac{\partial W}{\partial I2}\right) - \frac{\partial W}{\partial I2}\bar{\bar{F}}C\bar{\bar{F}}^{t} + \frac{\partial W}{\partial I3}I3\bar{\bar{F}}\bar{\bar{C}}^{-1}\bar{\bar{F}}^{t}\right)$$

Due to the form of B and C we have the following simplifications:

$$\bar{\bar{F}}C\bar{\bar{F}}^{t} = \bar{\bar{F}}\bar{\bar{F}}^{t}\,\bar{\bar{F}}\,\bar{\bar{F}}^{t} = \bar{\bar{B}}^{2}$$

$$\bar{\bar{F}}\bar{\bar{I}}\bar{\bar{F}}^{t} = \bar{\bar{B}}$$

$$\bar{\bar{F}}\bar{\bar{C}}^{-1}\bar{\bar{F}}^{t} = \bar{\bar{F}}\bar{\bar{F}}^{-1}\,\bar{\bar{F}}^{-t}\bar{\bar{F}}^{t} = \bar{\bar{I}}$$

$$\bar{\bar{\sigma}} = 2J^{-1}\left(\frac{\partial W}{\partial I3}I3\bar{\bar{\boldsymbol{I}}} + \left(\frac{\partial W}{\partial I1} + I1\frac{\partial W}{\partial I2}\right)\bar{\bar{\boldsymbol{B}}} - \frac{\partial W}{\partial I2}\bar{\bar{\boldsymbol{B}}}^{\boldsymbol{2}}\right)$$

Using the fact that I1 I2 and I3 are the invariant of B we have the following equation:

$$\bar{\bar{B}}^{3} - I1\bar{\bar{B}}^{2} + I2\bar{\bar{B}} - I3 = 0$$

Multiplying the equation by$\bar{\bar{B}}^{-1}$, we have:

$$\bar{\bar{B}}^{2} = I1\bar{\bar{B}} - I2\bar{\bar{I}} + I3\bar{\bar{B}}^{-1}$$

Replacing $\bar{\bar{B}}^2$ with its new expression in the previous form of $\bar{\bar{\sigma}}$:

$$\bar{\bar{\sigma}} = 2J^{-1}\left(\left(\frac{\partial W}{\partial I3}I3 + \frac{\partial W}{\partial I2}I2\right)\bar{\bar{\boldsymbol{I}}} + \left(\frac{\partial W}{\partial I1}\right)\bar{\bar{\boldsymbol{B}}} - \frac{\partial W}{\partial I2}I3\bar{\bar{\boldsymbol{B}}}^{-1}\right)$$

(2) Isotropic hyperelastic incompressible material:

The incompressibility traduced itself as:

$$I3 = 0$$

In order to take into account the incompressibility in the strain energy p is introduced as a Lagrange multiplier:

$$W(\bar{\bar{C}}) = W(I1, I2) + \frac{1}{2}P(I3 - 1)$$

The Piola stress becomes:

$$\bar{\bar{S}} = 2\frac{\partial W}{\partial \bar{\bar{C}}} + \frac{\partial P(I3 - 1)}{\partial \bar{\bar{C}}}$$

As done previously we differentiate W with respect to I1 and I2:

$$\bar{\bar{S}} = 2\frac{\partial W}{\partial I1}\bar{\bar{I}} + 2\frac{\partial W}{\partial I2}\left(I1\bar{\bar{I}} - \bar{\bar{C}}\right) + P\bar{\bar{C}}^{-1}$$

Using the same method as before the Cauchy stress has been calculated:

$$\bar{\bar{\sigma}} = \left(P\bar{\bar{\boldsymbol{I}}} + \left(2\frac{\partial W}{\partial I1}\right)\bar{\bar{\boldsymbol{B}}} - \frac{2\partial W}{\partial I2}\bar{\bar{\boldsymbol{B}}}^{-1}\right)$$

(3) Constitutive law the isolator: POLY-2P

Different model for the strain energy have been tested on ANSYS® . The criteria that have been used to choose the most reliable model were: convergence of the solution, accuracy of the solution respect to experimental results, verification of the principle of superposition.

The form that has been adopted is:

$$W = c_{10}(I1 - 3) + c_{01}(I2 - 3) + c_{20}(I1 - 3)^2 + c_{02}(I2 - 3)^2 + c_{11}(I1 - 3)(I2 - 3)$$

For an **incompressible material**, the principal stresses have the following form:

$$\bar{\bar{B}} = \begin{pmatrix} {\lambda^2}_1 & 0 & 0 \\ 0 & {\lambda^2}_2 & 0 \\ 0 & 0 & {\lambda^2}_3 \end{pmatrix}; \; \bar{\bar{B}}^{-1} = \begin{pmatrix} {\lambda_1}^{-2} & 0 & 0 \\ 0 & {\lambda_2}^{-2} & 0 \\ 0 & 0 & {\lambda_3}^{-2} \end{pmatrix}$$

$$\sigma_1 = \left(P + 2\frac{\partial W}{\partial I1}{\lambda^2}_1 - \frac{2\partial W}{\partial I2}{\lambda_1}^{-2} \right)$$
$$\sigma_2 = \left(P + 2\frac{\partial W}{\partial I1}{\lambda^2}_2 - \frac{2\partial W}{\partial I2}{\lambda_2}^{-2} \right)$$
$$\sigma_3 = \left(P + 2\frac{\partial W}{\partial I1}{\lambda^2}_3 - \frac{2\partial W}{\partial I2}{\lambda_3}^{-2} \right)$$

III. HDRB stress analysis:

A. Assessment of hyperelastic parameters:

In the precedent part we have seen that a hyperelastic law was characterized by a strain energy function. This function can have various forms (Mooney Rivlin, Poly-2P…). All these functions depends on parameters, these have to be determined to reproduce as well as possible the comportment of the material.

For the example the Poly-2P has the following strain energy function:

$$W = c_{10}(I1-3) + c_{01}(I2-3) + c_{20}(I1-3)^2 + c_{02}(I2-3)^2 + c_{11}(I1-3)(I2-3)$$

c_{10}, c_{01}, c_{20}, c_{02} and c_{11} are the parameters, they depend on the material that has to be model and should be chosen to fit the material behavior.

In order to determined these parameters standard tests have been defined: uniaxial tension test, uniaxial compression test, biaxial tension test, pure shear test, simple shear test, volumetric test. After a brief description of the different tests we will see how the tests to take into account have been chosen. Indeed it's not necessary to use all of them.

1. Standard tests:

The characteristic of the standard test will be given in function of the stresses σ_i and of the stretches λ_i , where:

$$\lambda_i = \varepsilon_i + 1$$

a) Uniaxial tensile test:

The aim of this test is to reach a state of pure tensile strain:

$$\sigma_2 = \sigma = \frac{P}{A};\ \ \sigma_1 = \sigma_3 = 0$$

$$\lambda_2 = \frac{L}{L_0};\ \lambda_1 = \lambda_3 = \sqrt{A/A_0}$$

To reach this state the specimen must be much longer in the load direction than in width and thickness dimensions (10 times approximately). The state will be reached in the middle of the specimen (where edge effects can be neglected).

The following pictures show the shape of the specimen and the kind of machine that can be use.

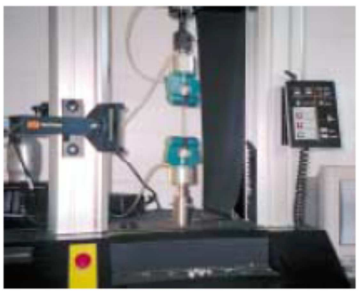

TENSILE MACHINE

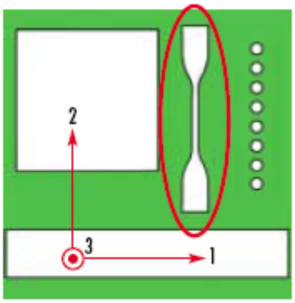

TENSILE SPECIMEN

b) *Biaxial tension test:*

The purpose of this experiment is to obtain the same state of strain in two directions:

$$\sigma_2 = \sigma_1 = \sigma;\ \ \sigma_3 = 0$$

$$\lambda_1 = \lambda_2 = \frac{L}{L_0};\ \lambda_3 = \frac{t}{t_0}$$

It can be reached by radial stretching of a disc; the machine and the specimen are successively presented:

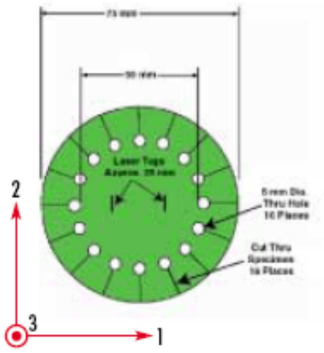

c) *Pure shear test:*

In order to create a pure shear state in the specimen, it is submitted to a very high tensile state. The geometry of the specimen, the width should be at least ten times the length, and the fact that the rubber is quasi incompressible create a pure shear state at 45° of the stretching direction. The state reached is :

$$\sigma_1 \neq 0\ ;\quad \sigma_2 = \sigma;\ \ \sigma_3 = 0$$

$$\lambda_1 = 1;\ \ \lambda_2 = \lambda\ ;\ \ \lambda_3 = \frac{\lambda^2 t}{t_0}$$

The following figures show the specimen and the experiment:

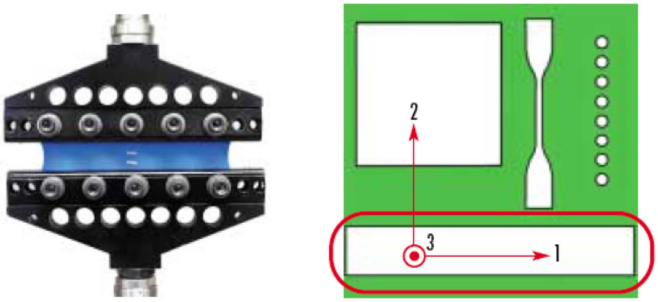

d) Simple shear test:

The state that is sought is shear in the direction 1/2. The specimen is deformed as shown on the following figure:

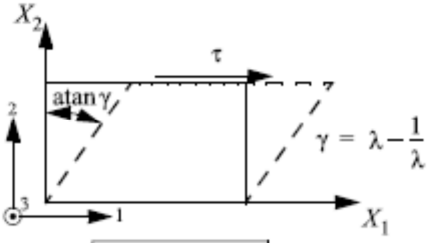

Stresses and strains take the following form:

$$\sigma_{12} = \tau = \frac{V}{A_0}$$

$$\lambda_1 = \lambda;\ \ \lambda_2 = \frac{1}{\lambda}\ ;\ \ \lambda_3 = 1$$

2. Fitting curves for the studied isolator:

The isolator that we are studying has the properties that were presented at the beginning. Thus it has a shear modulus G=1,4Mpa. All the tests we had at our disposition were made on the same rubber but with different shear modulus.

The following figures show the different tests linearly scaled to reach G=1,4Mpa, in fact the curves were simply multiplied by a factor λ (λ=1,4/G where G is the true shear modulus of the material tested).

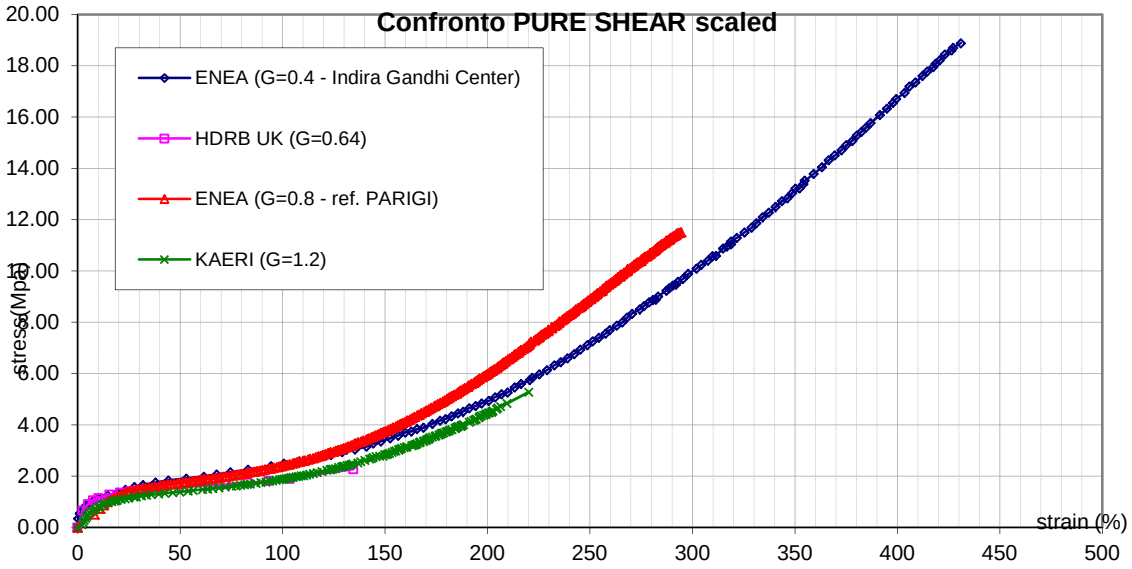
Confronto PURE SHEAR scaled
ENEA (G=0.4 - Indira Gandhi Center)
HDRB UK (G=0.64)
ENEA (G=0.8 - ref. PARIGI)
KAERI (G=1.2)
stress (Mpa)
strain (%)
20.00
18.00
16.00
14.00
12.00
10.00
8.00
6.00
4.00
2.00
0.00
0
50
100
150
200
250
300
350
400
450
500

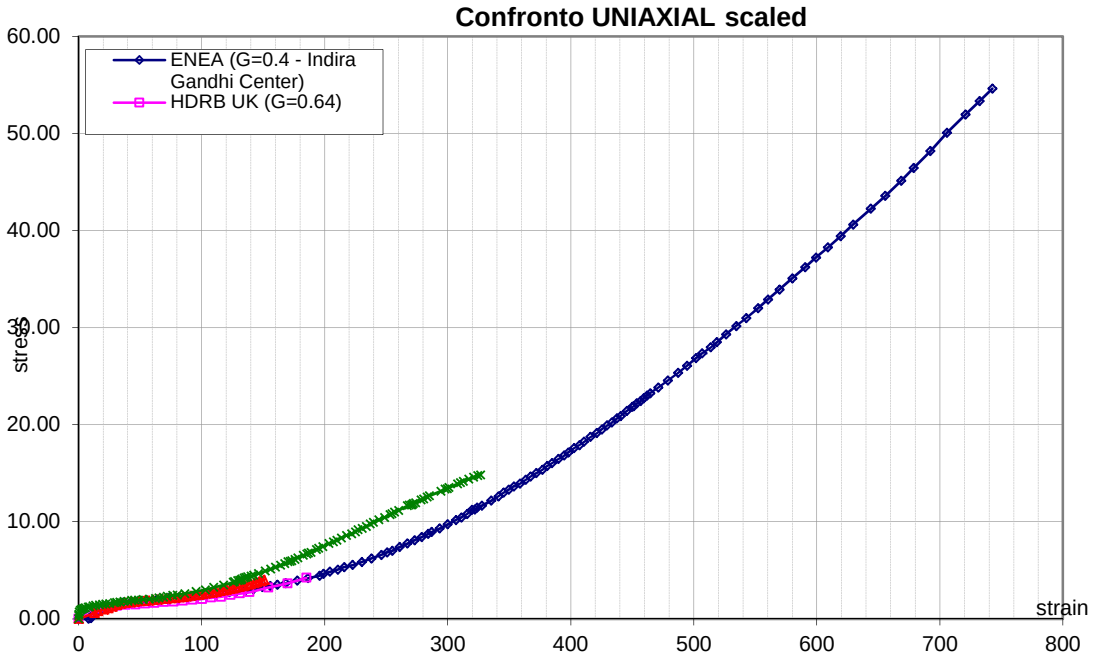
Confronto UNIAXIAL scaled
ENEA (G=0.4 - Indira Gandhi Center)
HDRB UK (G=0.64)
stress
strain
60.00
50.00
40.00
30.00
20.00
10.00
0.00
0
100
200
300
400
500
600
700
800

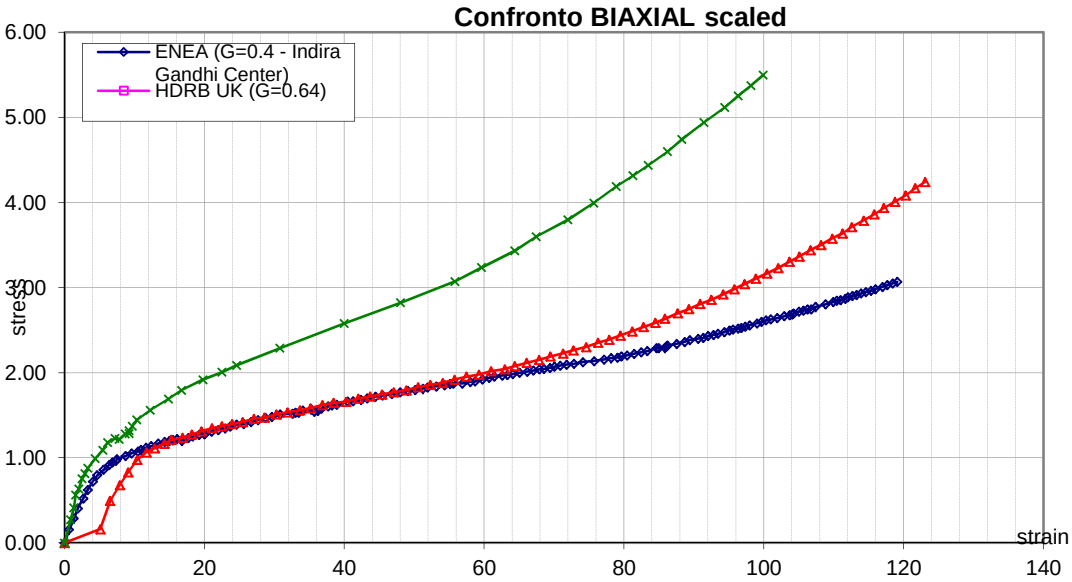

The linear scaling gives quite reasonable results and the method has thus been withheld to create the inexistent tests on the G=1,4Mpa rubber. Further developments should include a proper test battery.

The simple shear fitting test has been obtained thanks to the FIP horizontal load test on a 1/2 scaled isolator. Expect from the geometric scaling the tested isolator has all the proprieties of the real isolator.

The result of the test and the method used are shown on the following figures:

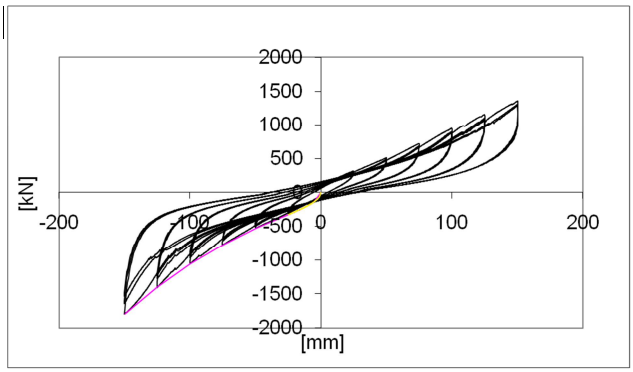

3. Choice of the optimal fitting:

Once all the curves are defined, we have to choose which combination of them we want to use. This choice has to be made on three criteria: the convergence of the solution, the accuracy of the fitting curves given by ANSYS® with respect to the input curves, the accuracy of the solution.

FITTING	TEST FITTATI					SFTW FIT	PARAMETRI POLY 2P								
	UNIAX	BIAX	SHEAR	S SHEAR	VOLUM		C10	C01	C20	C11	C02	D1	D2	Convergence	Accuracy of the solution
FIT_302	x	x	x	X		AN	0.79700	-0.05910	0.01609	-0.00529	1.103E-03	0.00000	0	ok	ok
FIT_306	x		x	X		AN	-0.89913	1.72189	-0.14567	0.88520	-7.301E-01	0.00000	0	no	
FIT_307	x	x		X		AN	0.68357	0.08819	0.03798	-0.06902	1.418E-02	0.00000	0	no	
FIT_308		x	x	X		AN	1.40172	-0.41017	-0.07215	0.08382	-1.105E-02	0.00000	0	ok	no

The accuracy of the fitting curves given by ANSYS® did not allow us to make a significant difference between the models and was acceptable for all of them.

The accuracy of the solution was based on criterion such has: effective vertical load close to the imposed one, pure horizontal load case corresponding to the simple shear fitting test, results close to the analytical solution for the vertical load.

B. Numerical model:

1. Model description:

The isolator is modeled through ANSYS® finite element software. Half isolator is modeled in its real dimension. The following characteristics of the model will be described: type of finite element, material proprieties, mesh generation, sensitivity of mesh to analysis, constraint of the model for upper and lower steel plates, constraint for symmetry, type of analysis, time and step divisions.

The model is shown on the following figure:

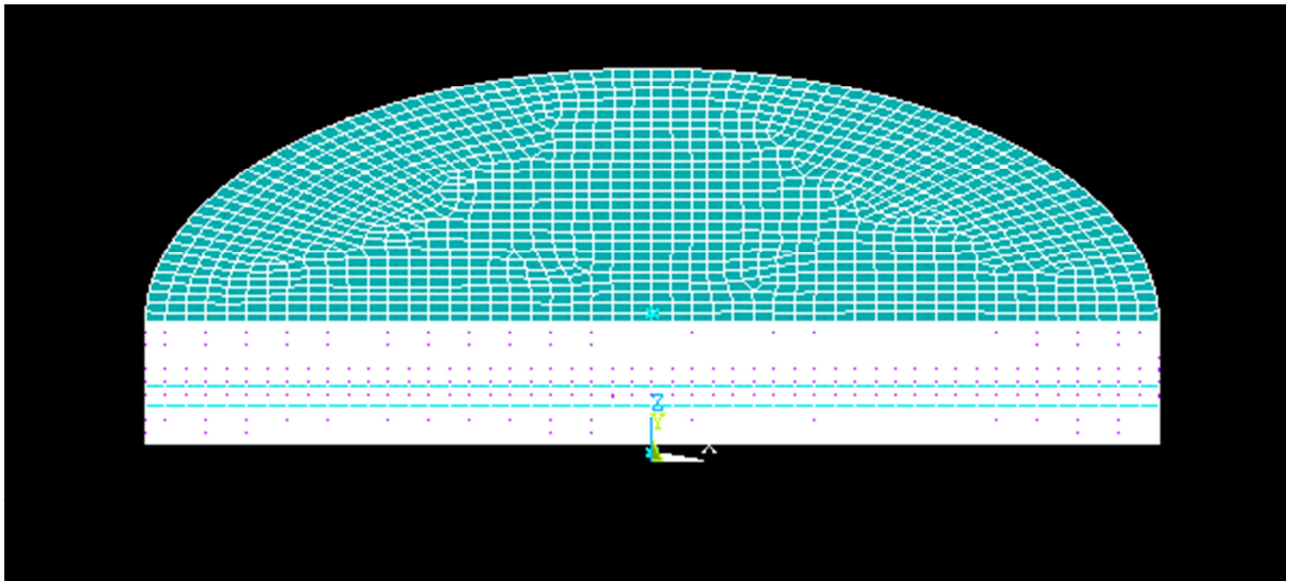

a) Finite element type:

The finite elements used in the model are: Solid 185, Shell 63, and MPC 184. After a description of their properties, their use will be exposed.

(1) Solid 185:

This element is used for the **rubber layer**. The element has 8 nodes; each node has three degrees of freedom that are the translations. It has two degenerated forms to allow irregular shapes as shown on the next figure:

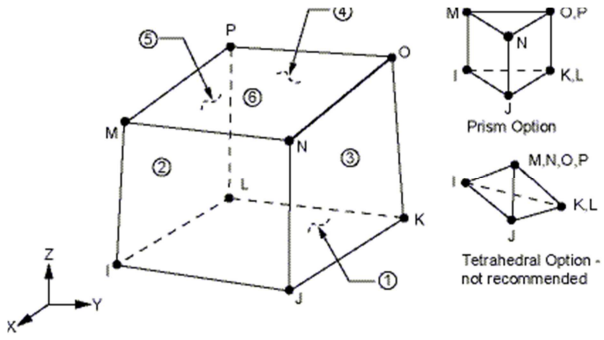

It's used in the following options: the hyperlastic constitutive law, non-layered solid. The pure displacement formulation is used. The integration is a uniform reduced integration with hourglass control; it helps preventing the volumetric locking for quasi incompressible materials as it has only one point of integration. This method of integration introduces some fictive energy regulated by a real constant. The solution is considered valid if the real energy and the final energy coincide within 5%.

(2) Shell 63 (thin shell):

This element is used to model the **steel layer**. The element has six degrees of freedom at each node: three translations and three rotations. It can be loaded weather in the in plane or in the normal direction. It can have both a membrane and a bending behavior. It has the following forms:

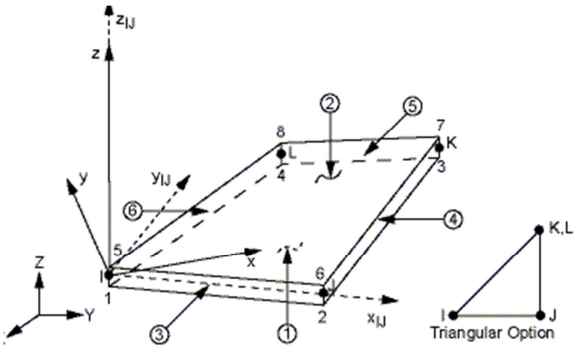

This element is used with the following options: both membrane and bending stiffness are activated. Large deflections effects are included and the stiffness matrix is approximated by the main tangent stiffness matrix. Extra displacement shapes are included, indeed the program automatically increase the stiffness of a small quantity to prevent the numerical instability of non warped elements.

(3) MPC 184:

This element is used to apply kinematics constraints between nodes. Here they create the **link** between the elements of steel and rubber. It exists of few types of element to apply those constraints; the rigid beam has been chosen to model a rigid constraint between two deformable bodies (the steel and rubber layers). This element transmits forces and moments. It's represented by the following figure:

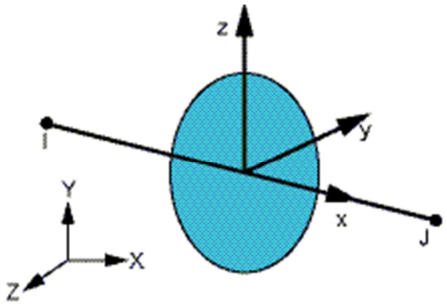

The rigid beam is used with the direct elimination method: kinematics constraints are imposed by multipoint constraints equations that are generated due to internal conditions. The dependent degrees of freedom are eliminated in favor of the dependant one.

b) Material properties:

The isolator is composed of two different materials: steel and rubber. The steel is considered as an elastic linear material whereas the rubber follows a hyperelastic law.

(1) Steel:

The steel is considered isotropic and is defined by its two constants: the young modulus (E=200000Mpa), the Poisson's ratio (ν=0,3).

(2) Rubber:

As said before the model used for the rubber is polynomial two parameters. The parameters have been obtained fitting the curves presented before with ANSYS®.

c) Mesh generation:

The first inferior rubber disc is created. First a circular area is created then meshed automatically, this automatic mesh is controlled by a dimensional parameter *es*. The area is extruded into a volume; the volume is composed of layers, the number of layers is controlled by a parameter *e* that can be modified easily to study the influence of the mesh on the solution.

The further layers of steel and rubber are alternately created at their respective heights with a cycle do. The layer of steel is created from a meshed area that has the thickness of a layer.

Each correspondent elements of the layer of steel and of rubber are finally linked with a rigid beam element.

d) Constraints:

The isolator is submitted to three constraints: the two external layers are rigidly linked to the externals steel plates; the isolator is symmetric and submitted to boundaries conditions.

(1) Rigid body constraint:

The two external layers of rubber are rigidly linked to the external steel plates which are both represented by a node situated on the barycenter of the plates.

(2) Symmetry constraints:

Only half isolator is represented as it has a symmetric behavior. To impose this symmetric behavior on the half isolator all the point located on radius where it has been cut (y=0) have the rotation around x and z and the translation along y blocked.

(3) Boundary conditions:

The isolator is totally constraint at its basis. The point that represents the basis steel plate is totally constraint. The point that represents the top plates is constraint in all rotations and in translation along y.

e) Analysis:

The software performs a static analysis where the large deflections and large deformations are permitted. The full Newton Raphson method is used to solve the non linear equations. The load is applied step by step. First the vertical load is applied (in 15 steps) then the horizontal displacement is imposed (in 40 steps) while the vertical load stays at its maximum. The loads are linearly interpolated step by step.

2. Global response of the model:

The global response of the model is first studied. Two situations are studied: the vertical and horizontal load. Applying a vertical the response the error is of the order of magnitude of $10E^{-4}$. The response to a horizontal displacement for the maximum and the minimum vertical load are compared to the simple shear test realized in the FIP laboratory:

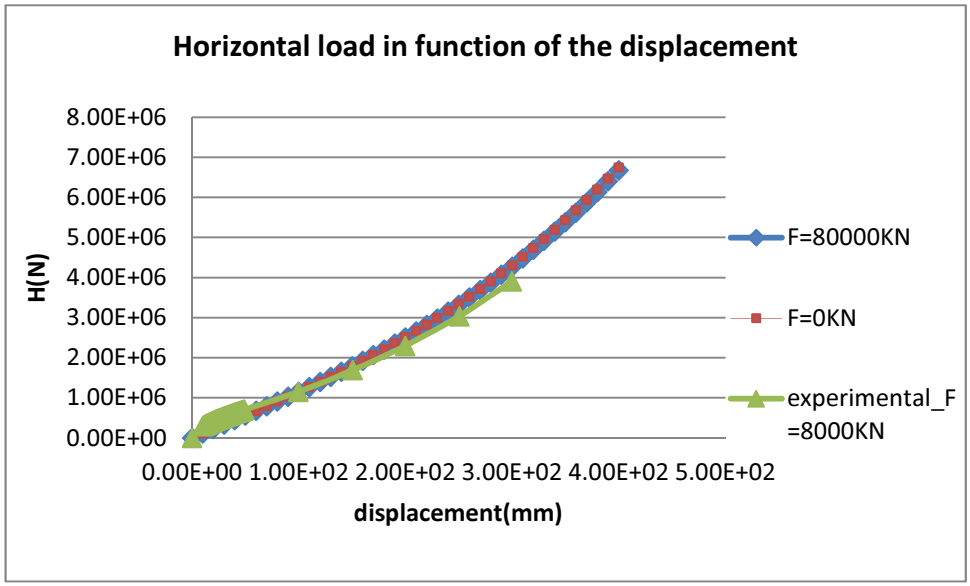

The correspondence between the model and the laboratory test is highly dependent on the parameters chosen in the constitutive law. The maximum error between the two curves is 8%, the global response of the model is accurate.

3. Mesh sensitivity:

The mesh sensitivity of the model has been studied in terms of global and local response. The main parameter of the mesh sensitivity is the number of subdivisions in one rubber layer, this parameter is called ***e.***

For reason of numerical cost the study of the mesh sensitivity has been realized on a **single layer**. However the comportment of a single layer and of the isolator has been compared.

The mesh sensitivity study is realized in the case of the **incompressible** rubber, the same comportments are observed in the compressible case.

It will be shown that the global response is not influenced by the choice of ***e*** whereas the local solution changes in a significant way.

a) Global response:

For a single layer the global response has been studied in three cases: e=4, e=10, e=16. The models were first loaded in terms of vertical load (10000KN), and then submitted to displacement until the 400% of the thickness of the rubber layer. The horizontal resultant was plotted in function of the displacement.

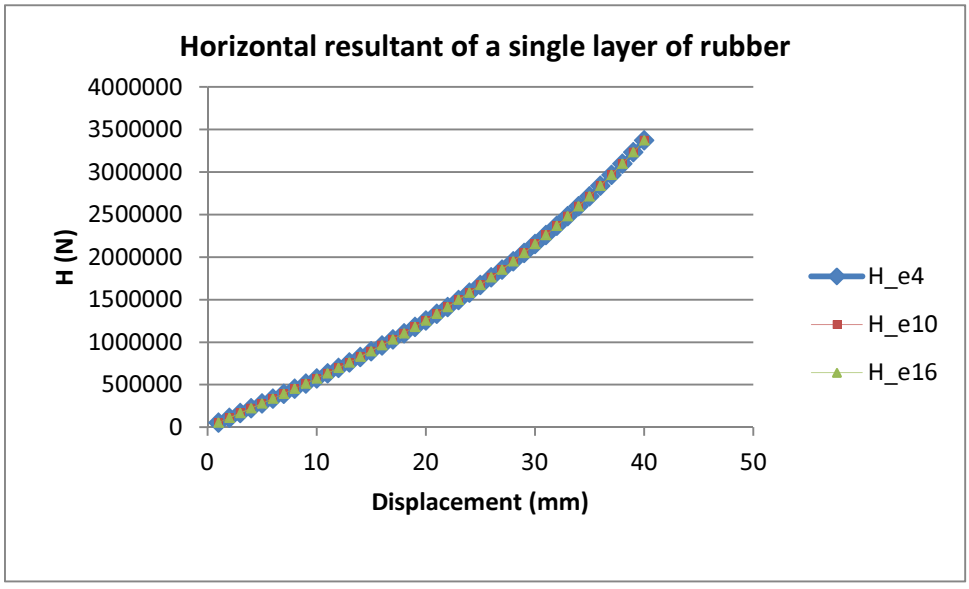

b) Local response:

The local response is studied in term of normal stress along the axis z (σ_z which is **negative for compression**) and tangential stress (τ_{xz}) for vertical and horizontal loads. This choice has been made since these stresses will be the one used in the definition of the failure domain.

We first study the response in terms of stresses for a **vertical load** of 10000KN:

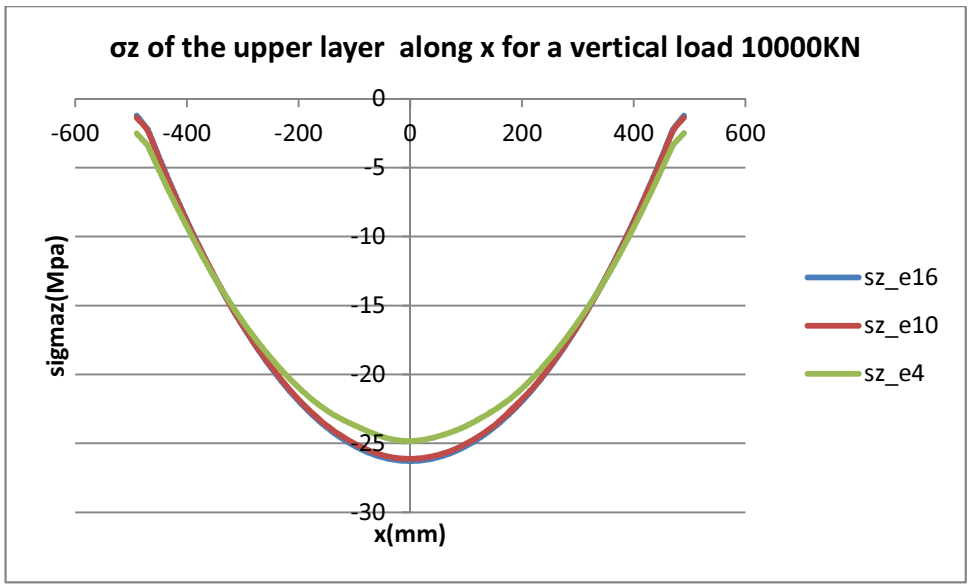

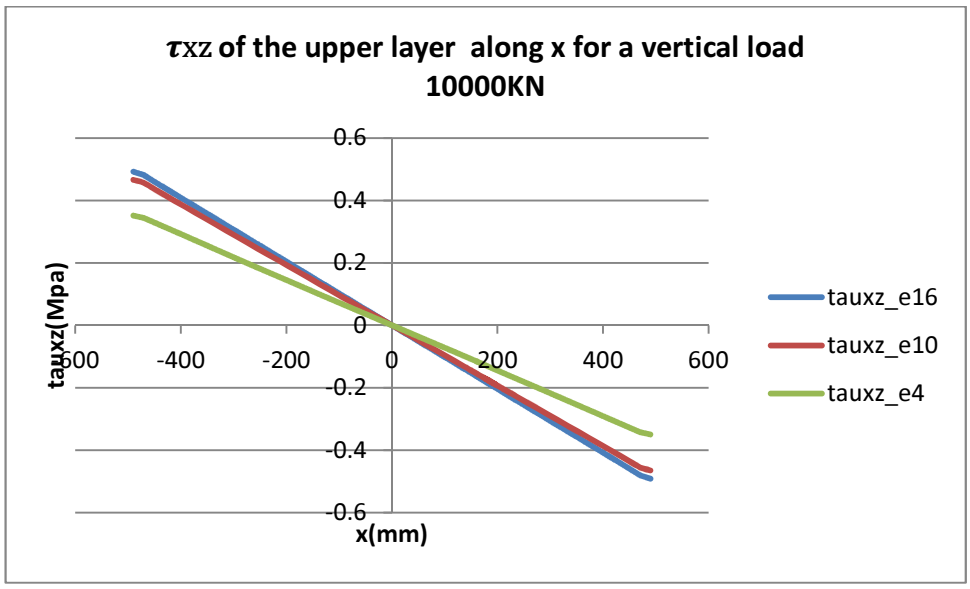

The shape of the stresses is not influenced by the mesh choice, however the modulus is. The solution converges when the number of layer is increasing.

The difference between τ_{xz} per e=4 and e=16 is 30%, this should be taken into account in further developments.

The local response has then been studied for a **horizontal load** that leads to a displacement of 300% of the rubber height:

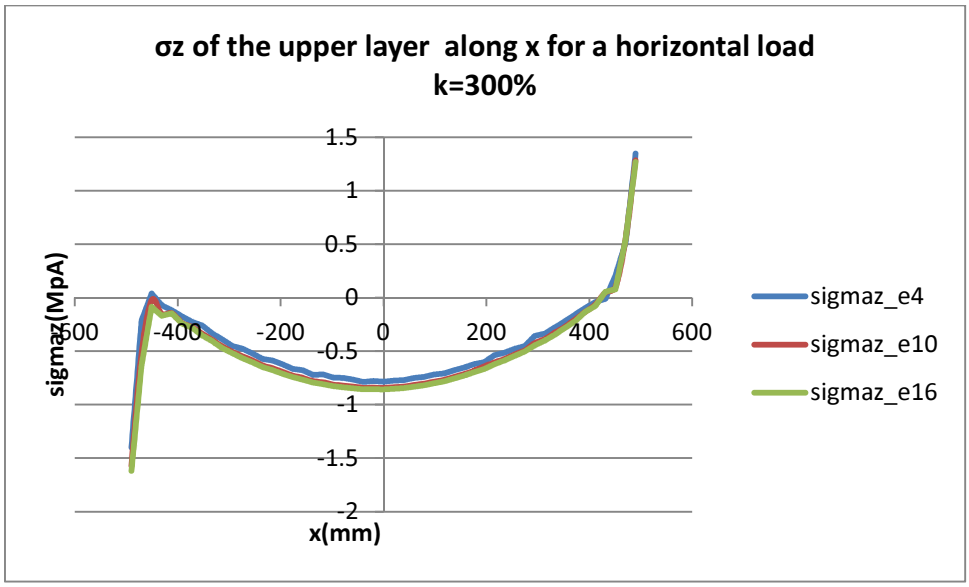

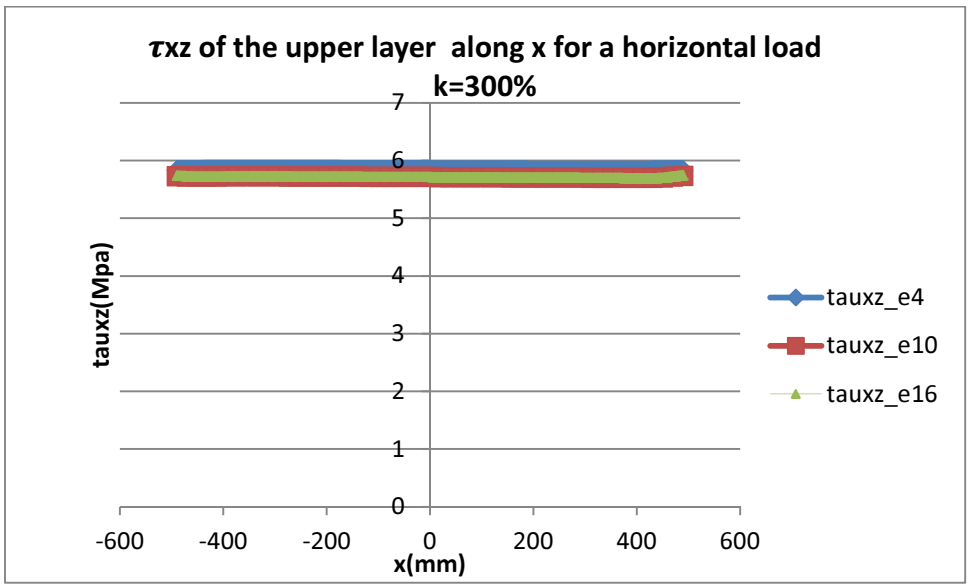

The mesh sensitivity due to the horizontal load is lower than due to the vertical load. The difference between the stresses for e=4 and e=16 is less than 10% for both normal and shear stresses.

In conclusion the only quantity with will be considered mesh dependent is **tauxz due to the vertical load**.

4. Incompressibility hypothesis:

Until now the material has been considered incompressible. The influence of the compressibility will be studied in the following paragraph.

The way compressibility has been introduced will be presented, the stresses will be compared and the correction coefficients that will be used to build a first approach of a domain with the compressible rubber will be calculated.

a) Compressible constitutive law:

The compressibility will be introduced trough the bulk modulus K. This bulk modulus will be used to build a volumetric test; this curve will be fitted in ANSYS® and allow us to find the two additive parameter of the poly2P constitutive law.

(1) Additive parameter of poly2P:

The strain energy for compressible rubber takes the following form:

$$Winc = c_{10}(I1-3) + c_{01}(I2-3) + c_{20}(I1-3)^2 + c_{02}(I2-3)^2 + c_{11}(I1-3)(I2-3)$$

$$Wcomp = Winc + \frac{1}{d_1}(J-1)^2 + \frac{1}{d_2}(J-1)^4$$

The parameters (d_1 and d_2) have to be defined. They depend only on the compressive behavior of the material, i.e. they depend only on the volumetric test and not on the other tests (biaxial, axial…).

(2) Bulk modulus K:

For nearly incompressible material the bulk modulus is much more representative of the material behavior. It can be expressed in function of the Poisson's ration ν and of the shear modulus G.

$$K = \frac{2G(1+\nu)}{3(1-2\nu)}$$

We have one data of one type of rubber that is used for HDRB. To have a reasonable range of compressibility variation we take K1=0,7Krubber and K2=1,3Krubber. I.e. K=2450 and K=4550.

(3) Volumetric test:

The bulk modulus is the slope of the volumetric test. The volumetric test is performed measuring the variation of volume of a sample submitted to a variation of pressure. The volume decreases when the pressure rises. We want to express the stress (that is this case is equal to the variation of pressure) in function of the volume strain J.

$$J = \frac{V}{V°}$$

We suppose the test linear. When the test starts the variation of pressure is zero and the volume strain is 1 as $V = V°$. We know that the slope is K we can deduce the following expression:

$$\Delta P = K - KJ$$

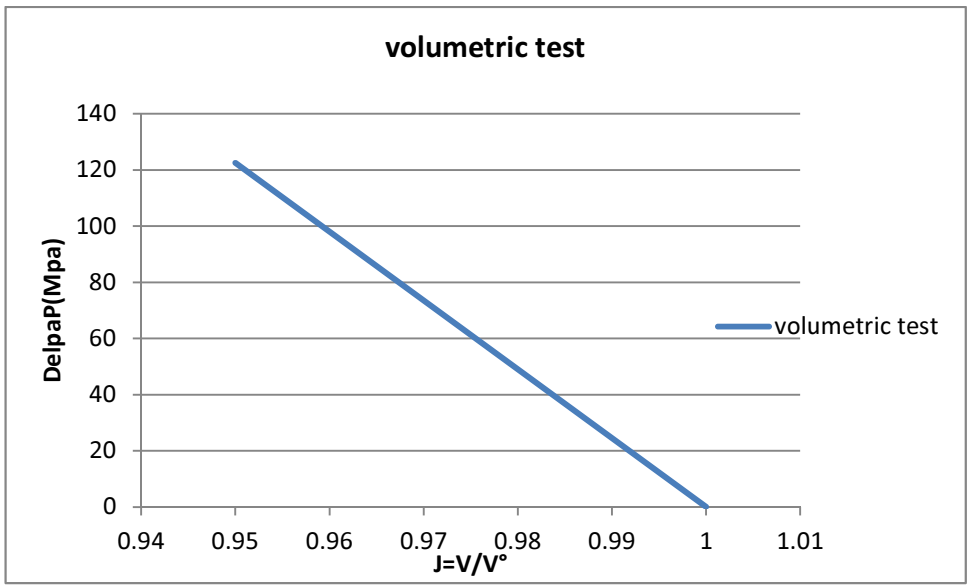

To identify the parameter of the polynomial hyperlastic law the hydrostatic part of the stresses deduced from the strain energy function are equalized to the pressure variation:

$$\sigma_{hydro} = -\frac{dW}{dJ} = \frac{-2}{d_1}(J-1) - \frac{4}{d_2}(J-1)^3 = \Delta P = -K(J-1)$$

We can now identify the parameter:

$$d1 = \frac{2}{K} \quad d2 = \infty$$

To impose the law in the software we take $d2 = 1000d1$

For the two bulk modulus chosen we have:

$$d1_{K2450} = 8{,}163E^{-4}\,\frac{\mathbf{mm^2}}{\mathbf{N}}$$

$$d1_{K4550} = 4{,}396E^{-4}\,\frac{\mathbf{mm^2}}{\mathbf{N}}$$

b) Stress comparison:

The stresses will be compared on the single layer model with 16 strata as it is the more accurate. The shear stress and normal stress along z will be compared for a vertical load of 10000KN and for a horizontal that correspond to k=3.

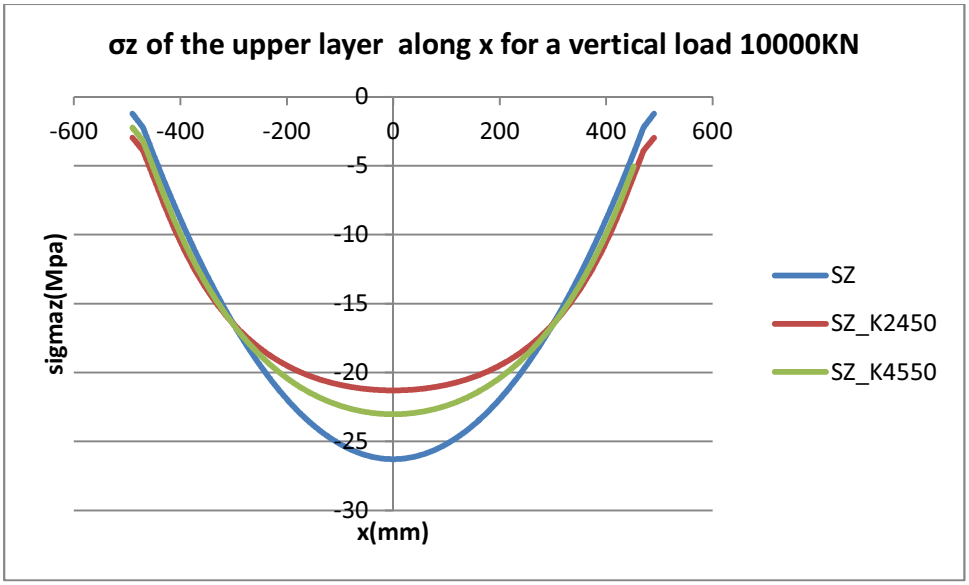

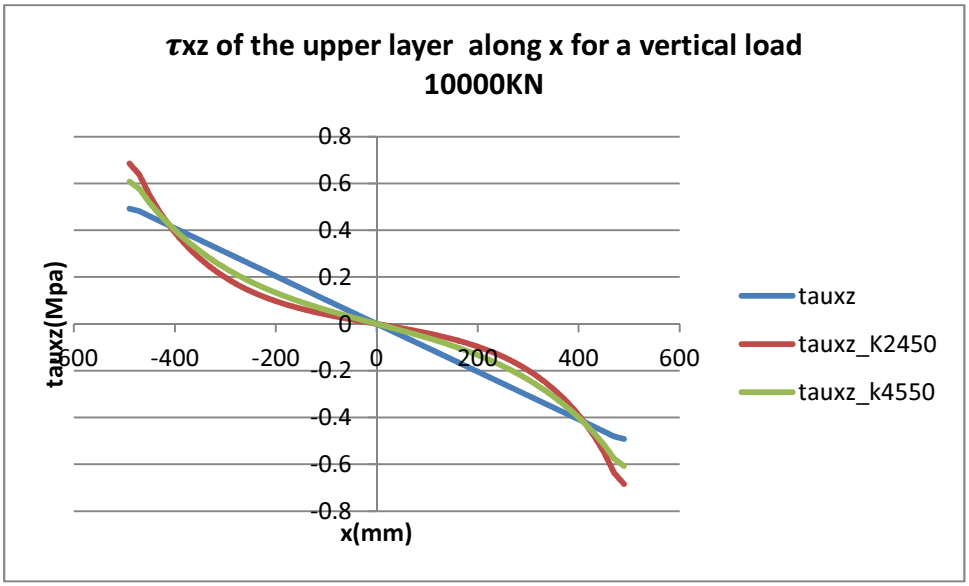
τxz of the upper layer along x for a vertical load 10000KN
tauxz(Mpa)
x(mm)
0.8
0.6
0.4
0.2
0
-0.2
-0.4
-0.6
-0.8
-600
-400
-200
0
200
400
600
tauxz
tauxz_K2450
tauxz_k4550

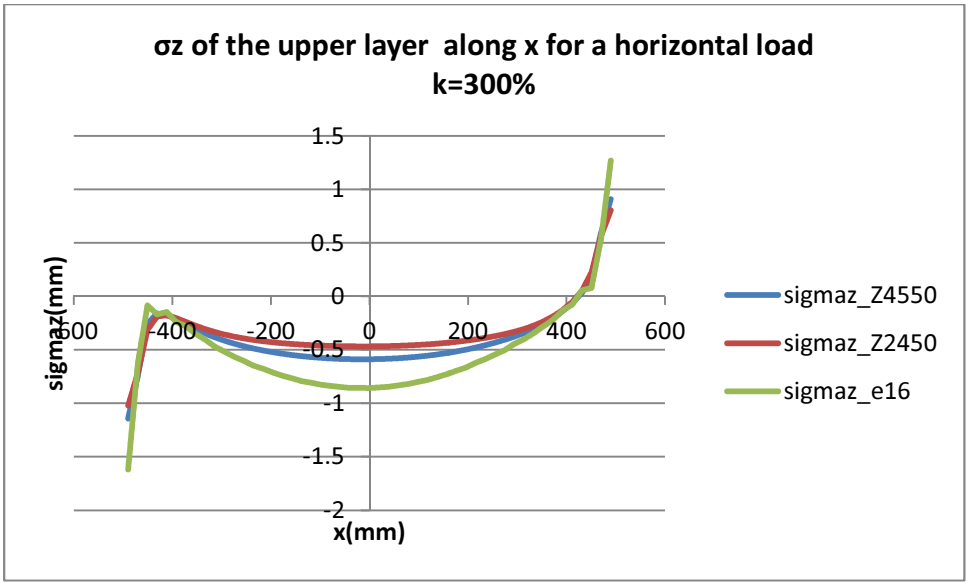
σz of the upper layer along x for a horizontal load k=300%
sigmaz(mm)
x(mm)
1.5
1
0.5
0
-0.5
-1
-1.5
-2
-600
-400
-200
0
200
400
600
sigmaz_Z4550
sigmaz_Z2450
sigmaz_e16

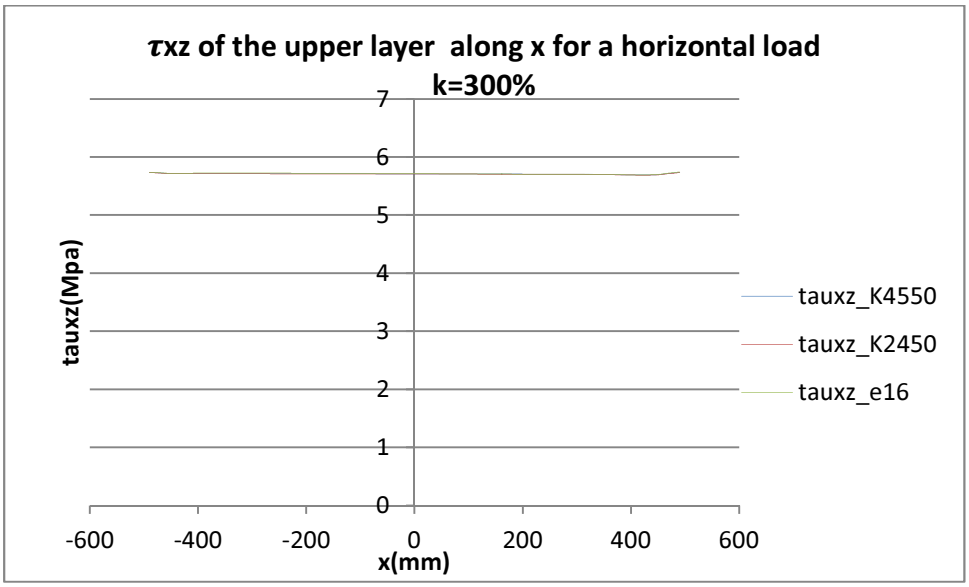
τxz of the upper layer along x for a horizontal load k=300%
tauxz(Mpa)
x(mm)
7
6
5
4
3
2
1
0
-600
-400
-200
0
200
400
600
tauxz_K4550
tauxz_K2450
tauxz_e16

The two quantities that are sensible to compressibility on the border are the normal stress due the horizontal load and the shear stress due to the vertical load. The normal stress due the vertical load is sensible on the center of the isolator but not so much on the border.

The general effect of compressibility is to absorb some of the compression by reducing the volume of the rubber. Therefore the compressions in the isolator are reduced.

c) Correction coefficients:

In order to analyze the effect of the compressibility on the domain the stresses that are influenced by this phenomenon will be modified. As the points that enter in the domain definition are on the border the stresses will be modified with a correction coefficient:

$$\tau_{xz_{vert-comp}} = \alpha \tau_{xz_{vert-incomp}} = \frac{\tau_{xz_{vert-comp-e16-border}}}{\tau_{xz_{vert-incomp-e16-border}}} \tau_{xz_{cert-incomp}}$$

$$\alpha_{K4550} = \frac{\tau_{xz_{vert-comp-e16-border}}}{\tau_{xz_{vert-incomp-e16-border}}} = \frac{0{,}60827}{0{,}49211} \cong 1{,}23$$

$$\alpha_{K2450} = \frac{\tau_{xz_{vert-comp-e16-border}}}{\tau_{xz_{vert-incomp-e16-border}}} = \frac{0{,}68544}{0{,}49211} \cong 1{,}4$$

$$\sigma_{z_{horcomp}} = \beta \sigma_{z_{hor-incomp}} = \frac{\sigma_{z_{hor-comp-e16-border}}}{\sigma_{z_{hor-incomp-e16-border}}} \sigma_{z_{hor-incomp}}$$

$$\beta_{K4550} = \frac{\sigma_{z_{hor-comp-e16-border}}}{\sigma_{z_{hor-incomp-e16-border}}} = \frac{1{,}1434}{1{,}6197} \cong 0{,}7$$

$$\beta_{K2450} = \frac{\sigma_{z_{hor-comp-e16-border}}}{\sigma_{z_{hor-incomp-e16-border}}} = \frac{1{,}0204}{1{,}6197} \cong 0{,}63$$

B. Analytical model:

In order to be able to handle the solution, in a first time the model has been created for **a layer of the rubber** that composes the seismic isolator. The normal stress due to the horizontal is really different for a single layer and for the **whole isolator,** a new model of stress that takes into account the behavior of the all isolator will be proposed.

The material will be considered **isotropic** and **incompressible**.

Two different approaches have been used: one for the vertical load case, one for the horizontal load case.

In the case of the vertical load the horizontal, displacements at stake can be considered small compared to the height. Thus we can apply the **small displacement** hypothesis and the material will be considered **elastic linear**. The horizontal displacement imposed to the isolator by the seism (horizontal load case) is on the contrary comparable to the height, indeed for the project load the isolator is designed to be able to deform itself until 300% of the height. Therefore the **finite deformation theory** will be used and the material will be considered **hyperelastic**.

In the analytical model stresses will be considered negative when of compression.

1. Stresses due to vertical load:

From a displacement model of a layer of rubber under a vertical load a stress model has been established. The hypotheses used are: small displacement, incompressible rubber, parabolic trend of the stresses along the radius, shear stress from this model equal of the shear stress found with incompressible model.

The following behavior has been considered concerning the way the rubber deforms itself under a vertical load:

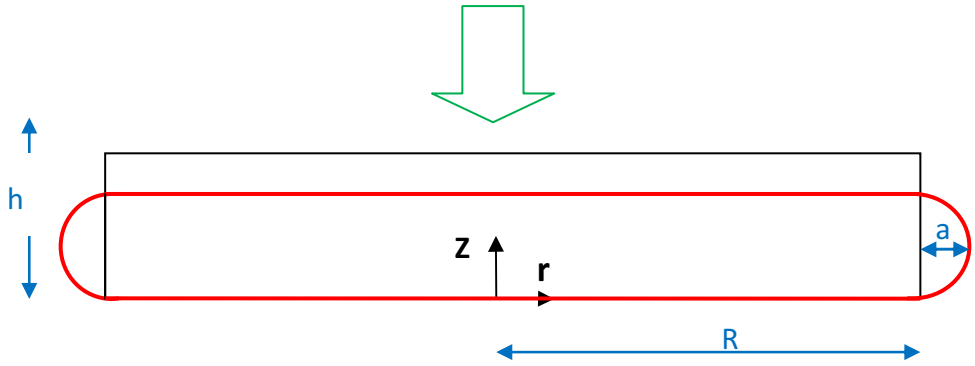

Figure 5 : Model of deformation of one layer of the rubber under vertical load

When the vertical load is applied the height of the rubber decreases and in the meantime the rubber overflows on the lateral part of the isolator.

We place ourselves in a cylindrical coordinates.

To describe this behavior we choose the following displacement model:

$$Sr(r,z) = \frac{ar}{R}\sin\left(\frac{\pi z}{h}\right)$$
$$S_\theta(r,z) = 0$$
$$S_z(r,z) = g(z)$$

Where the trigonometric function describes the overflowing behavior and the function g will be chosen to satisfy further requirement.

Thanks to the small displacement hypothesis and the compatibility equation, the normal and shear strains have the following form:

$$\varepsilon_r = \frac{\partial Sr}{\partial r} = \frac{a}{R}\sin\left(\frac{\pi z}{h}\right)$$
$$\varepsilon_\theta = \frac{1}{r}\left(\frac{\partial S_\theta}{\partial \theta} + Sr\right) = \frac{a}{R}\sin\left(\frac{\pi z}{h}\right)$$
$$\varepsilon_z = \frac{\partial Sz}{\partial z} = \frac{\partial g(z)}{\partial z}$$
$$\gamma_{rz} = \frac{\partial Sr}{\partial z} + \frac{\partial Sz}{\partial r} = \frac{ar}{R}\frac{\pi}{\mathrm{h}}\cos\left(\frac{\pi z}{h}\right)$$
$$\gamma_{z\theta} = \frac{1}{r}\frac{\partial S_z}{\partial \theta} + \frac{\partial S_\theta}{\partial z} = 0$$
$$\gamma_{r\theta} = \frac{\partial S_\theta}{\partial r} - \frac{S_\theta}{\mathrm{r}} + \frac{1}{r}\frac{\partial S_r}{\partial \theta} = 0$$

It has been supposed that in this case the rubber was incompressible. Therefore the first strain invariant has to be zero.

$$J_1 = \varepsilon_r + \varepsilon_\theta + \varepsilon_z = 2\frac{a}{R}\sin\left(\frac{\pi z}{h}\right) + \frac{\partial g(z)}{\partial z} = 0$$
$$Thus\colon \frac{\partial g(z)}{\partial z} = -2\frac{a}{R}\sin\left(\frac{\pi z}{h}\right)$$

Thanks to this hypothesis ($\varepsilon_r + \varepsilon_\theta + \varepsilon_z = 0$) the constitutive law adopts a simple form and the stresses are the following:

$$\sigma_r = P + 2G\varepsilon_r = \mathrm{P} + 2\mathrm{G}\frac{a}{R}\sin\left(\frac{\pi z}{h}\right)$$
$$\sigma_\theta = P + 2G\varepsilon_\theta = \mathrm{P} + 2\mathrm{G}\frac{a}{R}\sin\left(\frac{\pi z}{h}\right)$$
$$\sigma_z = P + 2G\varepsilon_z = \mathrm{P} - 4\mathrm{G}\frac{a}{R}\sin\left(\frac{\pi z}{h}\right)$$
$$\tau_{zr} = G\gamma_{rz} = G\frac{ar}{R}\frac{\pi}{\mathrm{h}}\cos\left(\frac{\pi z}{h}\right)$$

The value of the medium pressure has been determined through the vertical equilibrium. As the vertical displacement is free no reaction forces are created and we have the following equation:

$$-F = \int_A \sigma_z dA = \pi R^2(\ \mathrm{P(z)} - 4\mathrm{G}\frac{a}{R}\sin\left(\frac{\pi z}{h}\right))$$
$$Thus\ \mathrm{P(z)} = 4\mathrm{G}\frac{a}{R}\sin\left(\frac{\pi z}{h}\right) - \frac{F}{\pi R^2}$$

Along the radius the stress has been supposed parabolic, taking this hypothesis into account and replacing P by its formula founded previously we have:

$$\sigma_r = 2\left(6\mathrm{G}\frac{a}{R}\sin\left(\frac{\pi z}{h}\right) - \frac{F}{\pi R^2}\right)\left(\frac{R^2 - r^2}{R^2}\right)$$
$$\sigma_\theta = 2\left(6\mathrm{G}\frac{a}{R}\sin\left(\frac{\pi z}{h}\right) - \frac{F}{\pi R^2}\right)\left(\frac{R^2 - r^2}{R^2}\right)$$
$$\sigma_z = 2\left(-\frac{F}{\pi R^2}\right)\left(\frac{R^2 - r^2}{R^2}\right)$$

The constant a should now be determined. As done in the article another expression of the shear stress is found solving the differential equation that results from the incompressibility constraint:

$$\tau_{rz} = \frac{2Fhr}{\pi R^4}$$

Imposing that the two stresses coincide in z=0 and r=R:

$$\frac{Ga\pi}{h} = \frac{2Fh}{\pi R^3} \rightarrow a = \frac{2Fh^2}{\pi^2 R^3 G}$$

Finally we have the following expression of the stresses:

$$\sigma_r = -\frac{F}{\pi R^2}\left(2 - \frac{24h^2}{\pi R^2}\sin\left(\frac{\pi z}{h}\right)\right)\left(\frac{R^2 - r^2}{R^2}\right)$$

$$\sigma_\theta = -\frac{F}{\pi R^2}\left(2 - \frac{24h^2}{\pi R^2}\sin\left(\frac{\pi z}{h}\right)\right)\left(\frac{R^2 - r^2}{R^2}\right)$$

$$\sigma_z = -\frac{2F}{\pi R^2}\left(\frac{R^2 - r^2}{R^2}\right)$$

$$\tau_{zr} = \frac{2Fhr}{\pi R^4}\cos\left(\frac{\pi z}{h}\right)$$

2. Stresses due to horizontal displacement:

a) Corradi-Guiducci

In this part we will present a simple analytical model, further on it will be analyzed how this simple model fit the reality.

The isolator can be deformed horizontally until the 300% of its height. This cannot be considered a small displacement; therefore the analytical model will be based on the finite deformation theory.

Introducing a displacement model the stresses will be calculated trough this theory, the principal stresses will be first calculated. The incompressible formulation of principal stresses will be chosen and the pressure will be determined referring to the initial situation (no deformation). The final result depends on the constitutive law chosen; it will be introduced at last in order to enable an easy change of law.

A rubber layer has been taken into consideration; it has been assumed that it deformed itself like a parallelogram as shown on the figure:

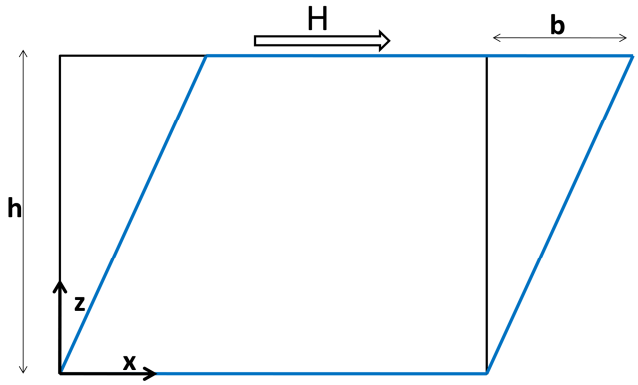

Figure 6: model of the deformation of a rubber layer under horizontal displacement

The displacement model in the Cartesian coordinates has therefore been assumed as:

$$s_x = \frac{b}{h} z = kz$$

$$s_y = 0$$

$$s_z = 0$$

The strain gradient has been deduced:

$$\bar{\bar{F}} = \bar{\bar{\mathrm{I}}} + \frac{\mathrm{ds}}{\mathrm{d}X_0} = \begin{bmatrix} 1 & 0 & \mathrm{k} \\ 0 & 1 & 0 \\ 0 & 0 & 1 \end{bmatrix}$$

Following the Lagrangian approach to determine the stresses created by the horizontal load, the left Cauchy Green tensor has been calculated:

$$\bar{\bar{B}} = \bar{\bar{F}}\bar{\bar{F}}^t = \begin{bmatrix} 1+\mathrm{k}^2 & 0 & \mathrm{k} \\ 0 & 1 & 0 \\ \mathrm{k} & 0 & 1 \end{bmatrix}$$

The hyperelastic law formulation is based on the value of the invariant of $\bar{\bar{B}}$. They can be easily expressed in function of the eigenvalues that will be consecutively calculated:

$$\lambda_1{}^2 = \frac{2 + k^2 + \sqrt{4k^2 + k^4}}{2}$$

$$\lambda_2{}^2 = 0$$

$$\lambda_1{}^2 = \frac{2 + k^2 - \sqrt{4k^2 + k^4}}{2}$$

The associated eigenvectors have the following form:

$$n_1 = \begin{bmatrix} \dfrac{k^2 + \sqrt{4k^2 + k^4}}{2k} & \dfrac{\sqrt{2}}{\sqrt{4 + k^2 + \sqrt{4k^2 + k^4}}} \\ 0 & \\ \dfrac{\sqrt{2}}{\sqrt{4 + k^2 + \sqrt{4k^2 + k^4}}} & \end{bmatrix}$$

$$n_2 = \begin{bmatrix} 0 \\ 1 \\ 0 \end{bmatrix}$$

$$n_3 = \begin{bmatrix} \dfrac{k^2 - \sqrt{4k^2 + k^4}}{2k} & \dfrac{\sqrt{2}}{\sqrt{4 + k^2 - \sqrt{4k^2 + k^4}}} \\ 0 & \\ \dfrac{\sqrt{2}}{\sqrt{4 + k^2 - \sqrt{4k^2 + k^4}}} & \end{bmatrix}$$

The expression of the invariant can be calculated:

$$I1 = {\lambda_1}^2 + {\lambda_2}^2 + {\lambda_3}^2 = 3 + k^2$$
$$I2 = {\lambda_1}^2{\lambda_2}^2 + {\lambda_1}^2{\lambda_3}^2 + {\lambda_2}^2{\lambda_3}^2 = 3 + k^2$$
$$I3 = {\lambda_1}^2{\lambda_2}^2{\lambda_3}^2 = 1$$

Principal stresses can now be determined with the relations established before and we will have:

$$\bar{\bar{\sigma}} = [n_1 \quad n_2 \quad n_3] \begin{bmatrix} \sigma_1 & 0 & 0 \\ 0 & \sigma_2 & 0 \\ 0 & 0 & \sigma_3 \end{bmatrix} \begin{bmatrix} {n_1}^t \\ {n_2}^t \\ {n_3}^t \end{bmatrix}$$

Principal stresses have been calculated with incompressibility assumption:

$$\sigma_1 = \left(P + 2\frac{\partial W}{\partial I1}{\lambda^2}_1 - \frac{2\partial W}{\partial I2}{\lambda_1}^{-2}\right)$$
$$\sigma_2 = \left(P + 2\frac{\partial W}{\partial I1}{\lambda^2}_2 - \frac{2\partial W}{\partial I2}{\lambda_2}^{-2}\right)$$
$$\sigma_3 = \left(P + 2\frac{\partial W}{\partial I1}{\lambda^2}_3 - \frac{2\partial W}{\partial I2}{\lambda_3}^{-2}\right)$$

Thus:

$$\bar{\bar{\sigma}} = \begin{bmatrix} P + 2\dfrac{\partial W}{\partial I1}k^2 + 2\dfrac{\partial W}{\partial I1} - 2\dfrac{\partial W}{\partial I2} & 0 & 2\left(\dfrac{\partial W}{\partial I1} + \dfrac{\partial W}{\partial I2}\right)k \\ 0 & P + 2\dfrac{\partial W}{\partial I1} - 2\dfrac{\partial W}{\partial I2} & 0 \\ 2\left(\dfrac{\partial W}{\partial I1} + \dfrac{\partial W}{\partial I2}\right)k & 0 & P + 2\dfrac{\partial W}{\partial I1} - 2\dfrac{\partial W}{\partial I2} - 2\dfrac{\partial W}{\partial I2}k^2 \end{bmatrix}$$

In order to determined P it has been assumed that the normal stresses should be zero when k=0, indeed this situation correspond to the initial situation when no displacement are imposed and thus no loads are applied.

$$P = -2\frac{\partial W}{\partial I1} + 2\frac{\partial W}{\partial I2}$$

$$\bar{\bar{\sigma}} = \begin{bmatrix} 2\frac{\partial W}{\partial I1}k^2 & 0 & 2\left(\frac{\partial W}{\partial I1} + \frac{\partial W}{\partial I2}\right)k \\ 0 & 0 & 0 \\ 2\left(\frac{\partial W}{\partial I1} + \frac{\partial W}{\partial I2}\right)k & 0 & -2\frac{\partial W}{\partial I2}k^2 \end{bmatrix}$$

The chosen constitutive law (Poly 2P) has a strain energy function of the following form:

$$W = c_{10}(I1-3) + c_{01}(I2-3) + c_{20}(I1-3)^2 + c_{02}(I2-3)^2 + c_{11}(I1-3)(I2-3)$$

Thus:

$$\frac{\partial W}{\partial I1} = c_{10} + 2c_{20}(I1-3) + c_{11}(I2-3) = c_{10} + 2c_{20}k^2 + c_{11}k^2$$
$$\frac{\partial W}{\partial I2} = c_{01} + 2c_{02}(I2-3) + c_{11}(I1-3) = c_{01} + 2c_{02}k^2 + c_{11}k^2$$

Finally we have:

$$\sigma_x = 2k^2(c_{10} + 2c_{20}k^2 + c_{11}k^2)$$
$$\sigma_z = -2k^2(c_{01} + 2c_{02}k^2 + c_{11}k^2)$$
$$\tau_{xz} = 2k(c_{10} + c_{01}) + 4k^3(c_{20} + c_{11} + c_{02})$$

All the stresses present a **uniform** pattern, i.e. they are constant in space and depend only on the state of deformation and on the material that compose the rubber.

The main assumptions that were made to reach this result were: **incompressibility** and **vertical restraint of the displacement**. These assumptions will be discussed when the results of analytical and numerical models will be compared.

b) Modified Corradi-Guiducci:

In the precedent model an artificial constraint has been introduced: the displacement along the axis z. Therefore the vertical resultant calculated as $\int \sigma_z dA$ is not zero.

The Corradi-Guiducci analytical solution is based on the behavior of a single layer. Comparing the behavior of numerical and analytical isolator we can note that: the shear stress does not depend on the interaction of the layers (all layer of the isolator can be considered as single layer) and the numerical and analytical model are in good agreement. Nevertheless the situation concerning the normal stress is different: the uniform analytical solution of the single layer is far from the numerical solution where we can see compression and traction zone. Furthermore the influence of the isolator behavior is big (the single layer solution is really different from the whole isolator one).

The traction behavior, that is very important for the definition of the domain, cannot be represented by the previous analytical model. A new model has been developed based on the general behavior observed on the numerical results. The model has been designed for the **all isolator** in the **principal plan**. The main hypothesis is that the **vertical resultant in this plan is zero**. The model has been developed for the **traction zone** as it's the one that matters in the domain definition.

The normal traction stress due to horizontal load depends on the value of the displacement k, on the height z of the point we are looking at in the isolator, on the abscissa x of the point. The chosen functions are out of phased with the height and the displacement.

The following form has been assumed:

$$\sigma_z = kcos\left(\frac{\pi x}{R} + \frac{k\pi}{3R}\left(z - \frac{H}{2}\right)\right)$$

The resultant on the principal plan is zero as the wave length is R.

This solution is compared to the numerical solution for traction zone ($x\epsilon[0, R]\ z\epsilon[\frac{h}{3}, h]$). This comparison is effectuated on the half isolator for z=H, z=H/2 for different displacement (k=2, 3, 4). The second traction zone ($x\epsilon[-R, 0]\ z\epsilon[0, \frac{2h}{3}]$) has the same behavior that is ensure by the term $\left(z - \frac{H}{2}\right)$.

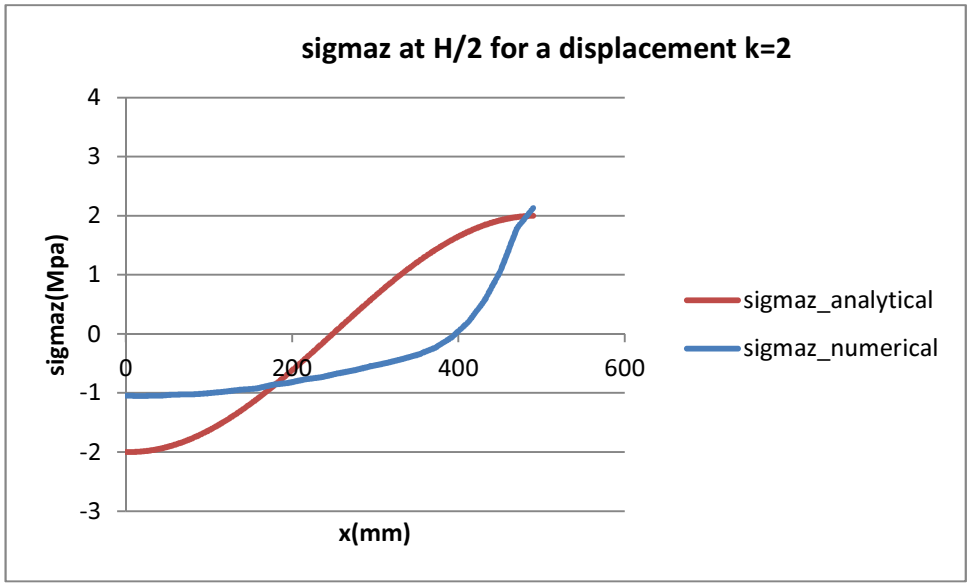
sigmaz at H/2 for a displacement k=2
sigmaz(Mpa)
x(mm)
sigmaz_analytical
sigmaz_numerical

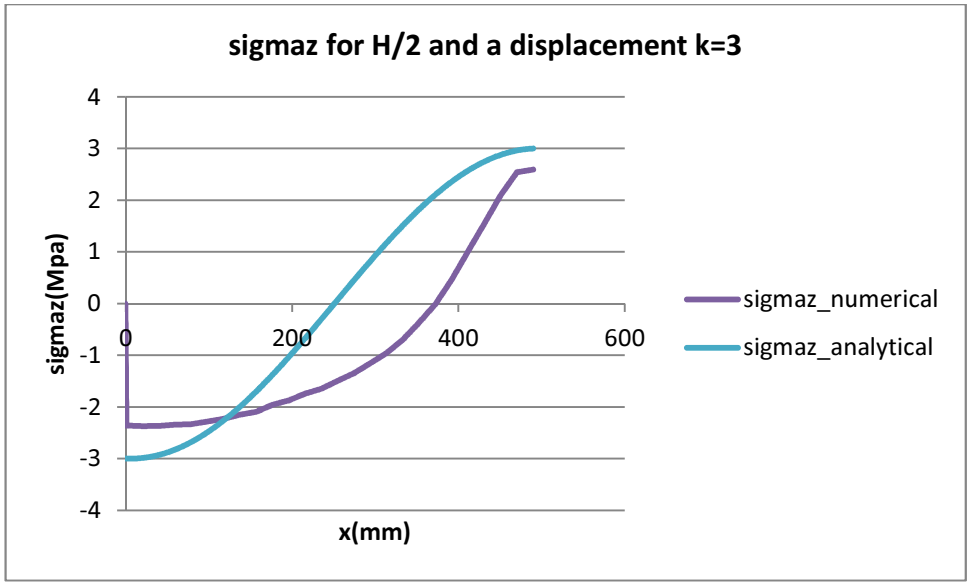
sigmaz for H/2 and a displacement k=3
sigmaz(Mpa)
x(mm)
sigmaz_numerical
sigmaz_analytical

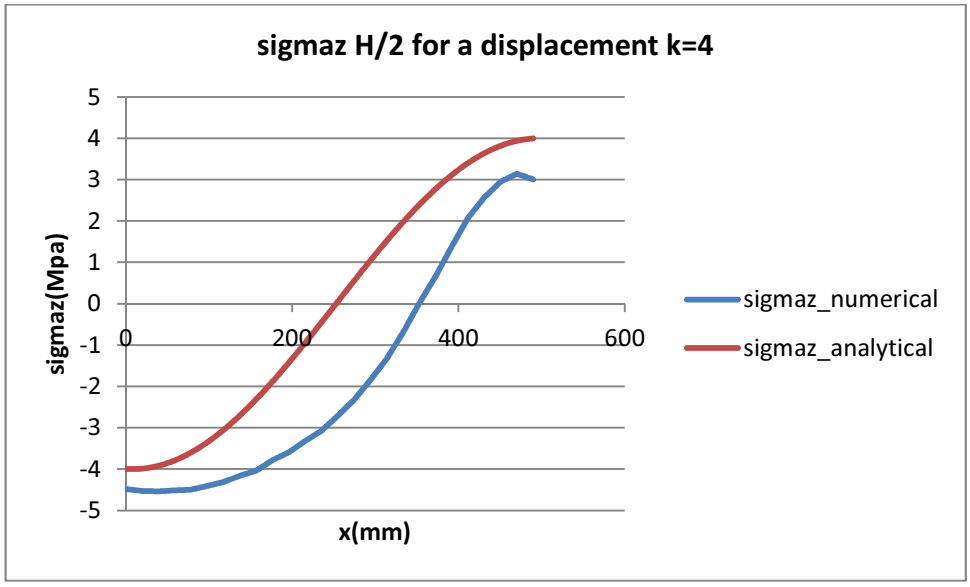
sigmaz H/2 for a displacement k=4
sigmaz(Mpa)
x(mm)
sigmaz_numerical
sigmaz_analytical

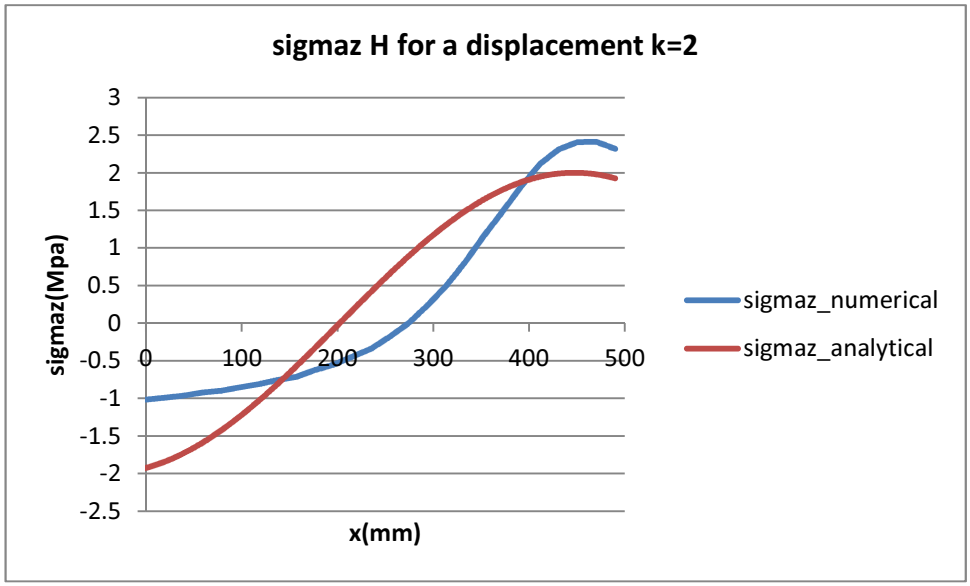

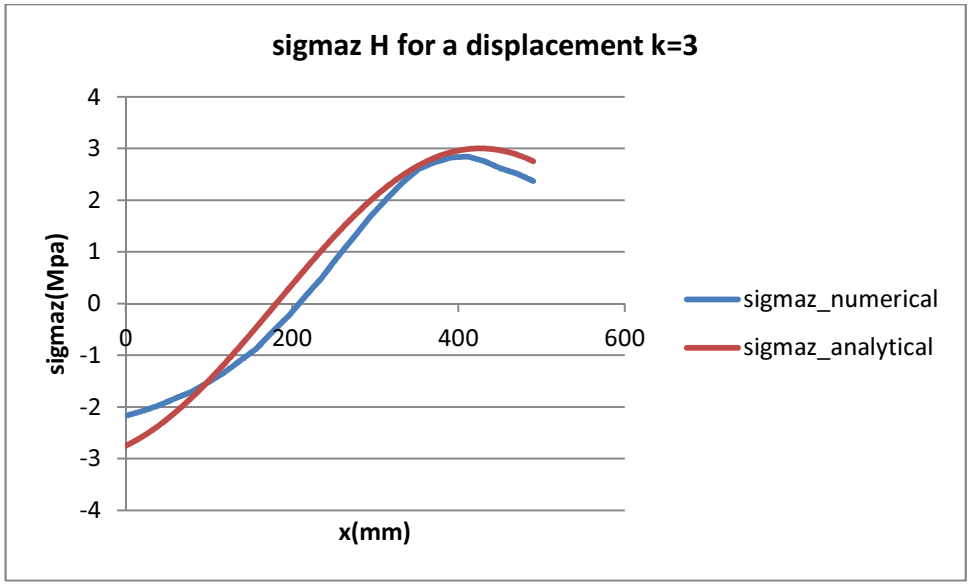

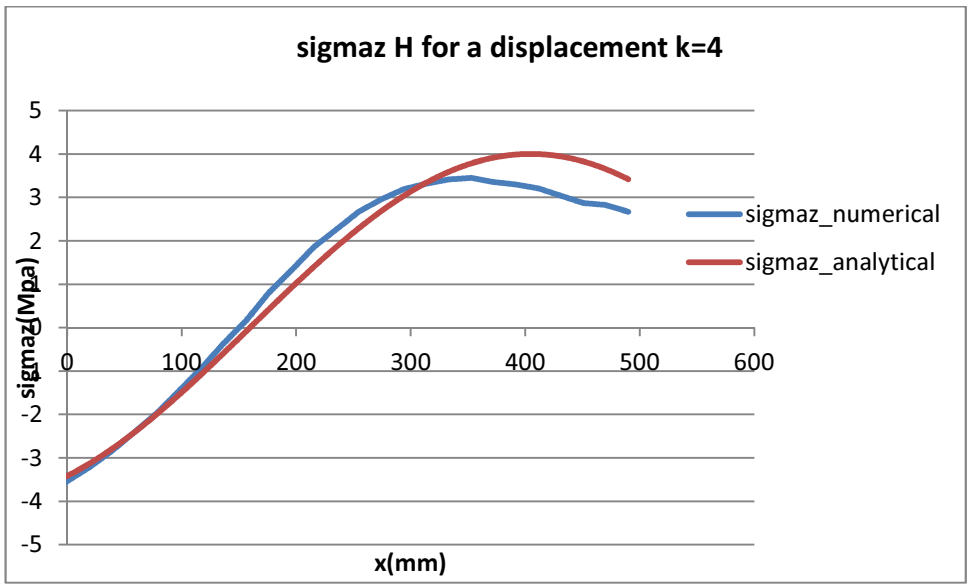

The general trends and the maximum value on the border are coherent; the model is not perfect but is a great step forward compared to the uniform solution.

C. Comparison – analytical and numerical models:

The models would be compared in their local and global behavior, thus in terms of stresses and resultant.

1. Global behavior

The global behavior of the **whole isolator** is studied. The horizontal resultant of the numerical model is plotted for two different vertical loads: no vertical load (V=0KN) and the maximum vertical load (V=80000KN). In both case a displacement along the horizontal of 400% of the rubber height is imposed. Those two responses are compared to the analytical model. In the analytical model the horizontal resultant is calculated from the τ_{xz} due to the horizontal load, a uniform trend of τ_{xz} along x has been hypothesized.

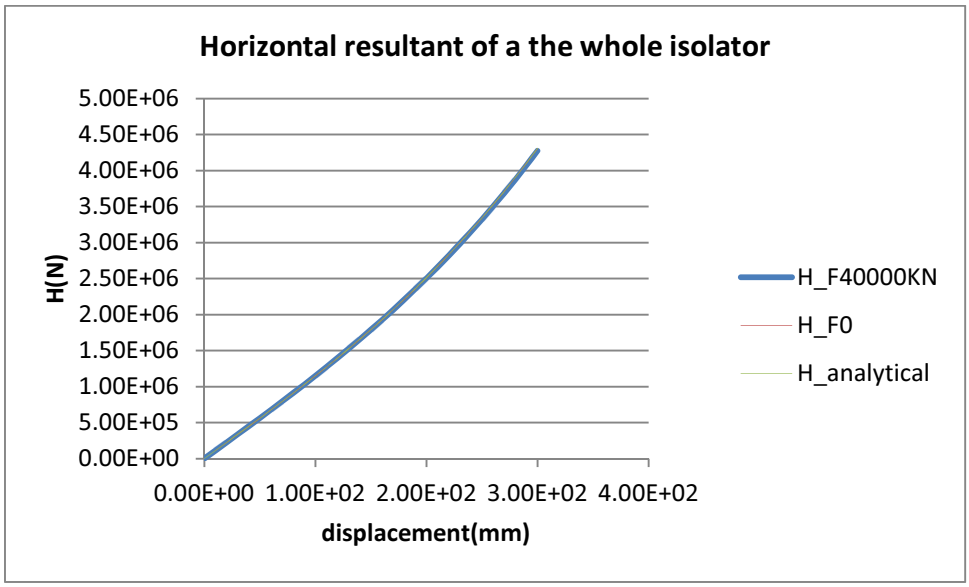

The different curves cannot really be distinguished from each other on the graphic; the horizontal global response is accurate.

2. Local behavior

The analytical model calculates σ_{z_vert}, τ_{xz_vert} and τ_{xz_hor} reasoning on a single rubber layer, while σ_{z_hor} reflects the behavior of the all isolator. The three first quantities will be compared for a single layer and then for a layer in the isolator. The rubber is considered incompressible; the same trends appear for compressible rubber.

a) Single layer:

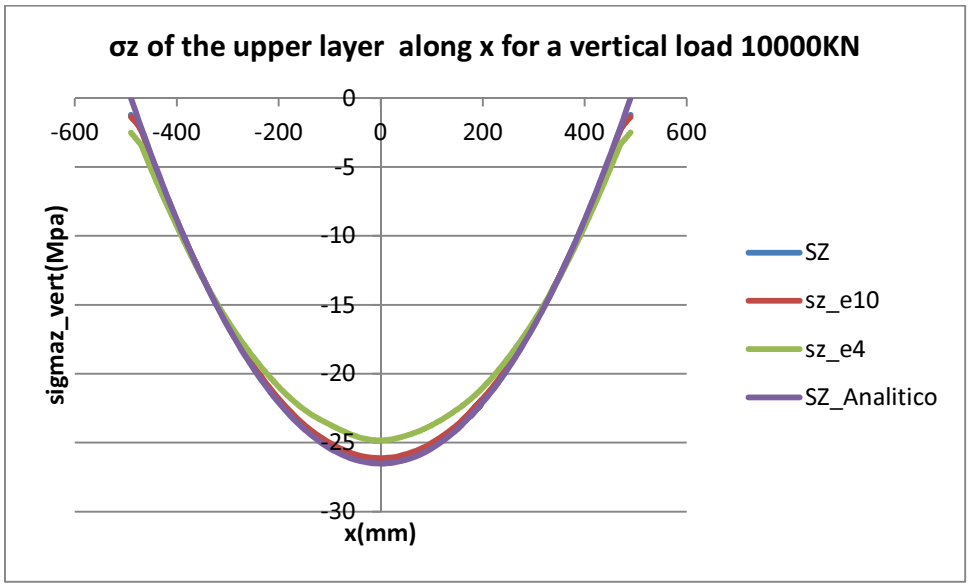

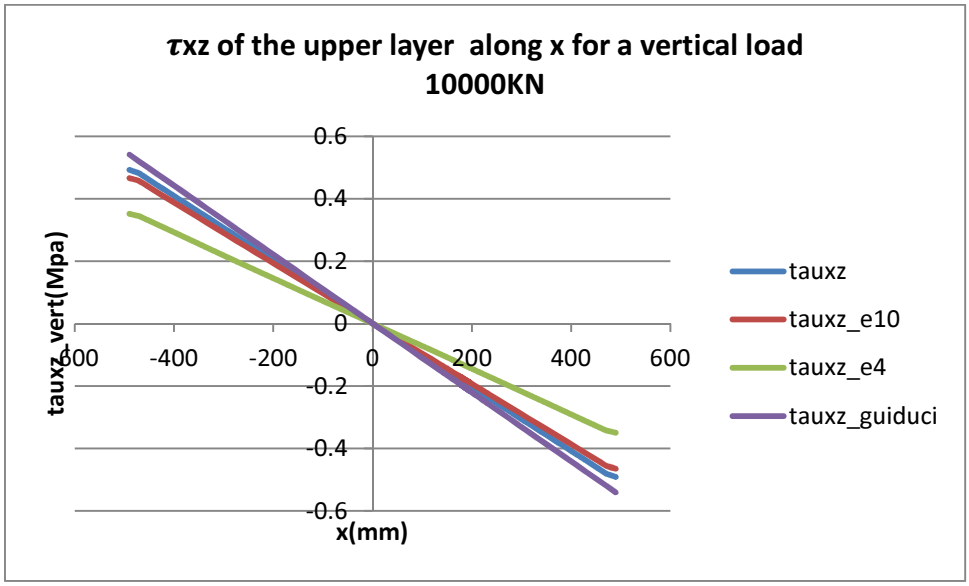

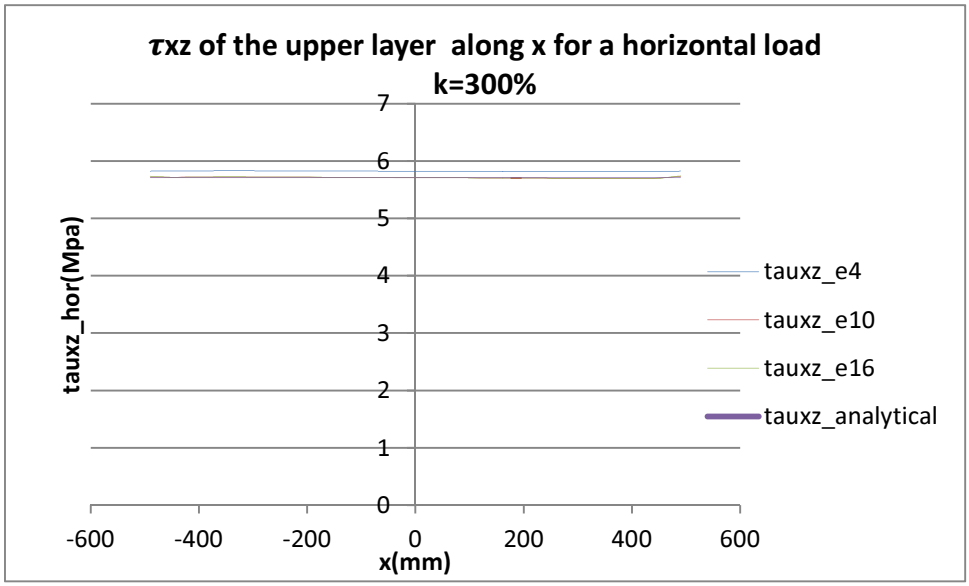

The analytical and numerical solutions match very well for a single layer, furthermore we had noticed that the numerical solution converge when the mesh is refined, indeed it converges toward the analytical solution.

b) Whole isolator:

The study will be carried on the whole isolator, for reason of numerical cost the e was chosen equal to 4. The solution the upper layer of the isolator and of the single rubber layer will be compared to the analytical solution.

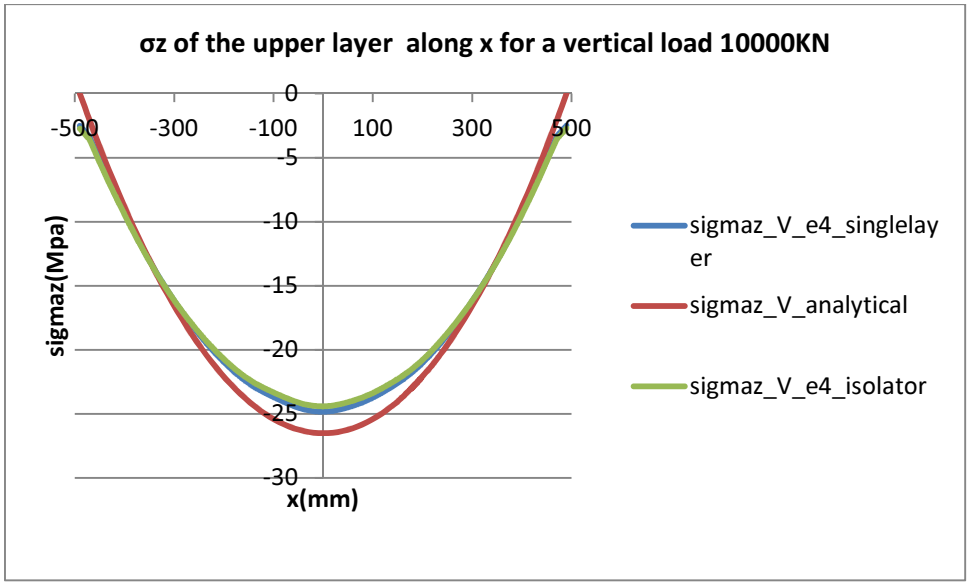

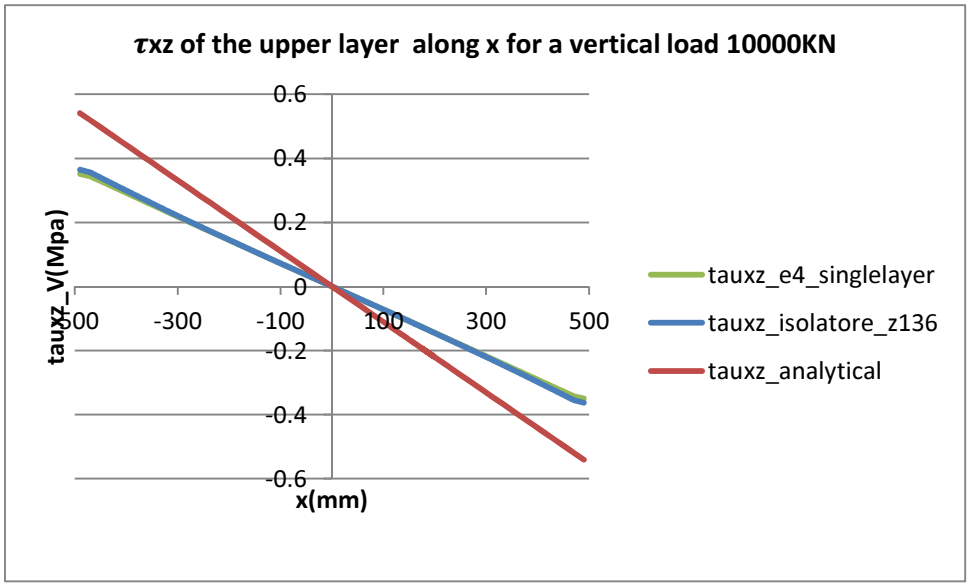

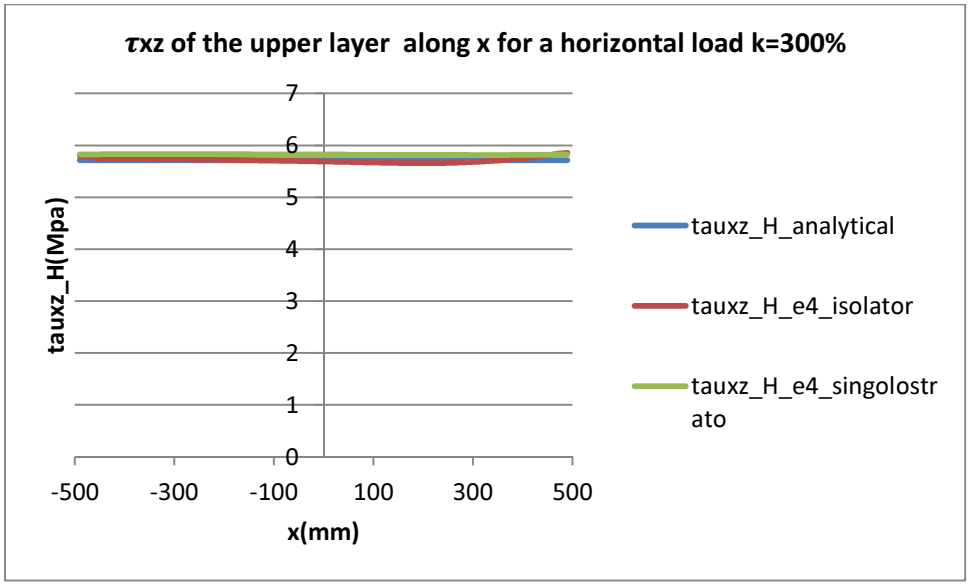

The single layer solution and the whole isolator solution can be considered equal for those three stresses, thus $\boldsymbol{\sigma_z}$ **due to the horizontal load is the only stress influence by the interaction between layers**.

To illustrate this fact the following picture represents the τ_{xz} due to the vertical load in the different layers of the rubber:

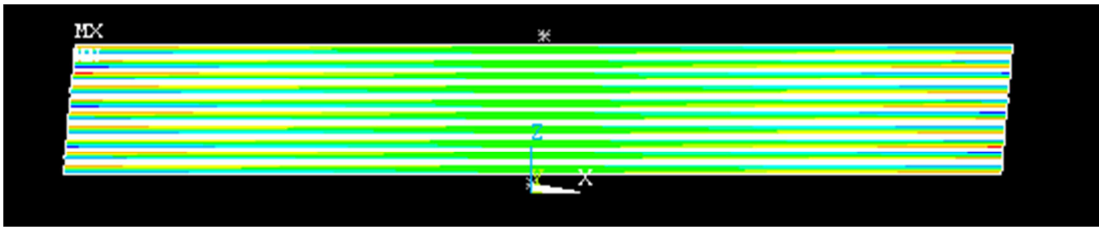

We can therefore apply the conclusions found in the single layer study: $\boldsymbol{\sigma_z}$ due to the vertical load and τ_{xz} due to horizontal load match between analytical and numerical model. τ_{xz} due to the vertical load converge to the analytical solution when the mesh is refined.

IV. HDRB limit state domain:

A. Definition of the studied failure mode:

In the conditions of strains and temperature that we are confronted to the rubber can be considered non-crystallized.

1. Delamination:

The delamination is the only studied failure mode that is linked to the whole isolator behavior. The behavior of the isolator is ensured by the interaction between the rubber and steel layer. If the two layers are detached in a certain zone the proprieties of the isolator are drastically reduced.

In delamination our isolator is seen as a composite material. It can be assumed that it follows the failure criterion established for the composites introducing the limit parameters of our material.

The phenomenon is shown on the following figure:

Schematic view of delamination

2. Tensile rupture:

The four following rupture modes are only linked to the material properties. The ultimate tensile strength is the maximum stress the material can withstand while being stretched or pulled before necking (when the section starts contracted).The ULS is usually found performing a tensile test and recording the stress and the strain. The highest point of the stress strain curve is the ULS.

This property is a characteristic of the material and does not depend on the size on the sample. Nevertheless it depends on factor such as: the surface state of the sample, temperature.

3. Tearing:

The tearing rupture occurs when the material is broken apart without the help of a cutting tool. This phenomenon is govern by the function *G* called strain energy released rate. G is the energy released during the propagation of the fracture per unit of new surface created by the rupture. If the energy available is greater than G_c (the critical energy), the crack spreads. This critical energy is a material property, usually independent of the loads applied and of the solid geometry.

It has been showed that in our case G depend on the tearing rate and the temperature. It is also sensible to visco-elastic properties, nevertheless changes in visco-elastic properties can be traduced in terms of tearing rate and temperature variations. Thus the sensibility is only studied for the two first quantities. G increases with the tearing rate and decreases with temperature.

4. Fatigue:

Fatigue can be observed in a material when progressive weakening of material properties occurs (like stiffness). It's a local failure provoked by variation of stresses or strains over time. It's a three-phase rupture mechanism: the initiation of the crack, the propagation and the rupture.

Fatigue proprieties depend on many factors as: geometry, surface quality, temperature. Square holes and sharp corners leads to elevate local stresses; surface roughness create local concentration of stresses; this local state of stress favors the fatigue mechanism. High and low temperature can also accelerate the phenomenon.

The characteristics of this phenomenon have not yet been entirely studied on rubber or in an empirical way; the only well established quantity is the mechanical limit fatigue which is the stress condition where fatigue can't happen in any reasonable time.

5. Cavitations:

The cavitation is the infinite expansion of empty cavities trapped in the rubber during its formation and the vulcanization process. This expansion occurs when a critical hydrostatic tension is reached.

The stability of the cavities has been studied in a linear case, but this theory does not give satisfying theory for our material which is highly non linear.

Even if the stability is satisfied the study of the cavities size can be of first interest for the tearing mode or the fatigue mode where the size of the initial crack is an essential data.

6. Localization of the failure:

a) Numerical model:

We have the following schematic form of stresses:

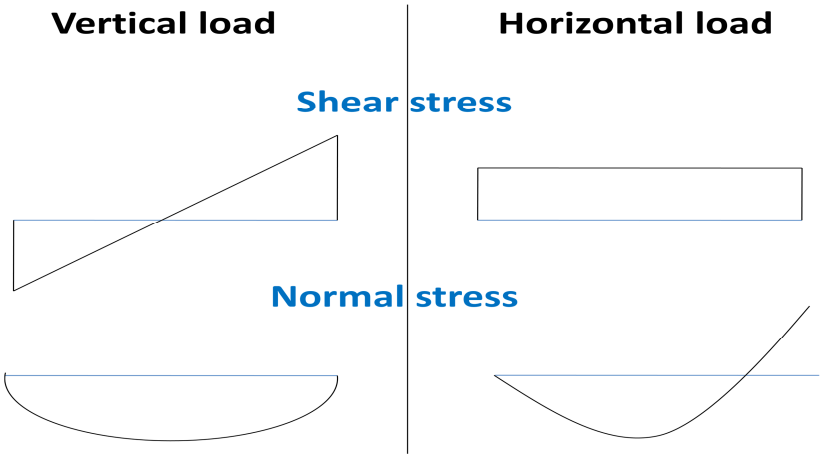

The first damage will happen in the zone where the total shear stresses are the higher; from the previous figure we can see that the maximum stress will be reach on the border of the isolator.

At equivalent shear stress, the failure will occur first in the traction zone if it exits. The border points that are in traction for a pure horizontal load situation (the vertical load makes the tractions decreased) will be chosen.

b) Analytical model:

We have the same schematic forms of the stresses; for the reason of maximum shear we select the point on the upper strata of the rubber layers:

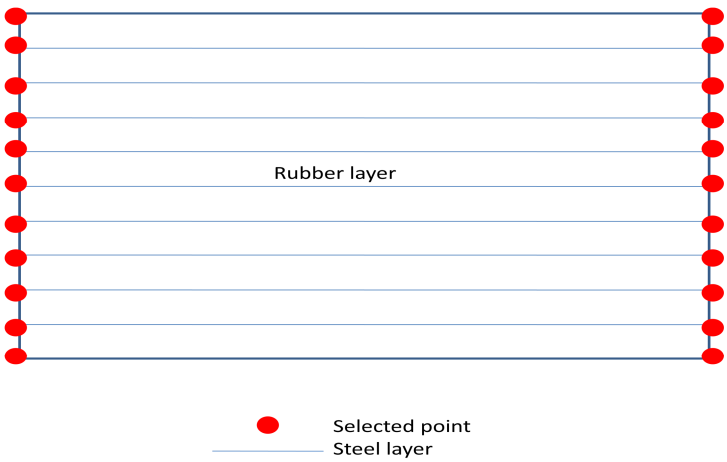

At equivalent shear stress, the failure will occur first in the traction zone if it exits. We will choose the point with the highest traction stress on the border.

B. Mohr-Coulomb model for delamination:

1. Theoretic definition of the domain:

Yen and Caiazzo have been modeling the **delamination** failure of both unidirectional and fabric composites. Our isolator is made of alternative layers of steel and rubber. The layer are made of isotropic materials (in the case of fabric composites, the fabric cannot be considered isotropic), thus our isolator can be considered as a unidirectional composite.

The axis number 3 is defined as the one perpendicular to the layers of the composite as shown on the figure. With this convention the criterion takes the following form:

$$\left(\frac{\sigma_{3T}}{S_{3T}}\right)^2 + \left(\frac{\tau_{13}}{S_{130} + S_{SR}}\right)^2 = 1$$

$$S_{SR} = \sigma_{3C} * f$$

$$\sigma_{3T}: tensile\ stress\ along\ the\ axis\ 3$$

$$\sigma_{3C}: compression\ stress\ along\ the\ axis\ 3$$

$$\tau_{13}: shear\ stress$$

$$S_{3T}: through\ the\ thickness\ tensile\ strength$$

$$S_{130}: reference\ shear\ strength$$

$$f: internal\ friction\ factor$$

We can decompose this criterion in two parts: the tensile and the compression part. Under tensile load the criterion becomes:

$$\sigma_{3C} = 0 \rightarrow S_{SR} = 0$$

$$\left(\frac{\sigma_{3T}}{S_{3T}}\right)^2 + \left(\frac{\tau_{13}}{S_{130}}\right)^2 = 1 \rightarrow \tau_{13} = S_{130}\sqrt{1 - \left(\frac{\sigma_3}{S_{3T}}\right)^2}$$

The effect of the compressive load is taking into account according to the Mohr-Coulomb theory:

$$\sigma_{3T} = 0$$

$$\left(\frac{\tau_{13}}{S_{130} + \sigma_{3C} * f}\right)^2 = 1 \rightarrow \tau_{13} = S_{130} + \sigma_3 * f$$

Therefore the σ/$\boldsymbol{\tau}$ failure domain due to the phenomenon of delamination has the following shape:

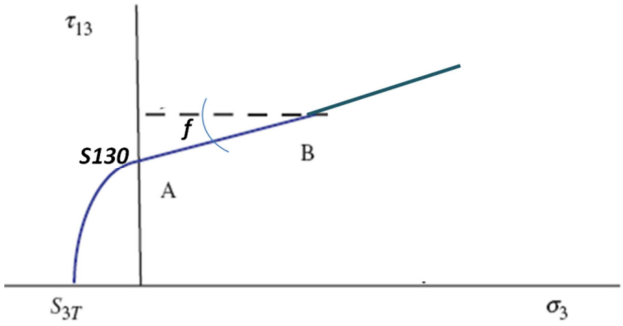

2. Determination of the constants of the domain:

a) Presentation of the methods used:

We want to define a first damage domain, i.e. when for the first time one element of the all isolator can be considered in failure, when the failure starts.

To define the domain as presented before we have to determine three constants: S_{130}, S_{3T}, f. We will first describe the test that can be use to determine these constant and then explain how the test have been taken into account in order to define a first ply domain.

S_{3T} is the tensile stress reached when there is no shear stress, it can be determined stretching a specimen of the rubber until the first signs of degradation appear.

S_{130} on the contrary occurs for a state of pure shear. Referring to the analytical model that has been presented before, we assume that for a vertical load on the edge of the isolator (r=R) and on the top of the rubber layer (z=h) we have the following state of stress:

$$\sigma_z = 0$$

$$\tau_{rz} = \frac{2Fh}{\pi R^3}$$

Therefore the limit strength S_{130} will be determined as the shear stress reached in this point under a compression load that leads to the first sign of failure.

Due to a lack of data on the isolator the Mohr-Coulomb friction coefficient f, will be considered zero. This assumption ensure safety standards as in compression S_{130} is always reached before $S_{130} + \sigma_3 * f$. On further developments the value of f should be sought.

b) Determination of S_{3T}:

The producer furnishes the tensile strength to be 17,5Mpa.

c) Determination of S_{130}:

We have to determine when the first signs of failure are reached in our isolator when it is submit to a compression load. A compression test on the scaled ½ isolator has been performed, the results are presented in the following figure:

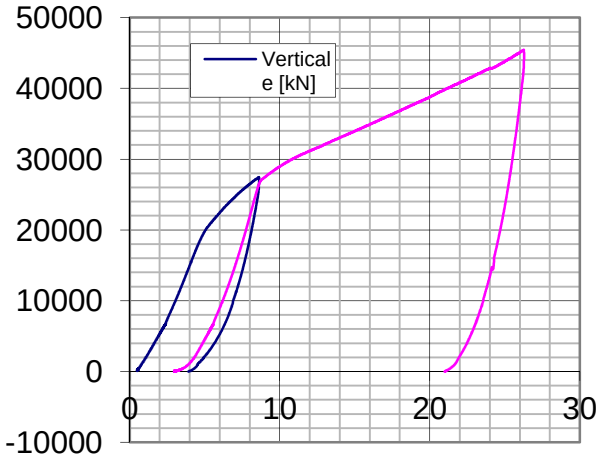

This graph represents the behavior of the isolator under a compression load, this is a global behavior. We have to find out what are the signs on the global behavior that indicates that on a local point of view the crisis has started.

We can simplify the constitutive law of the rubber in the following way:

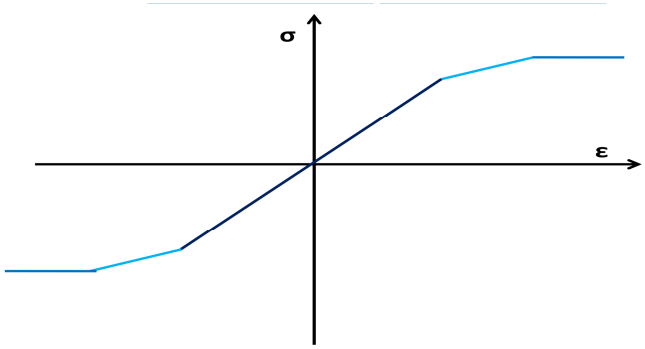

We can now traduce this local behavior in term of global behavior tracing the moment curvature graphic:

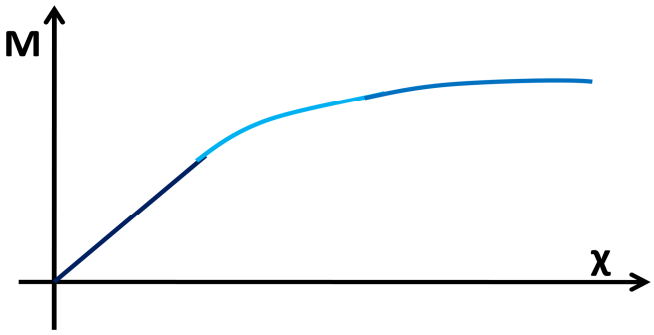

The three different parts of the curves in the local scale are represented by the same colors in the global scale. The transition from one slope to another in the local scale traduces itself by a change of curvature in the global scale.

In the local scale the first ply occurs when the yield limit is reached (first change of slope), this traduce itself in the global scale by a change of curvature. Therefore the first ply limit is reached in the global approach **as soon as the behavior is not linear anymore**.

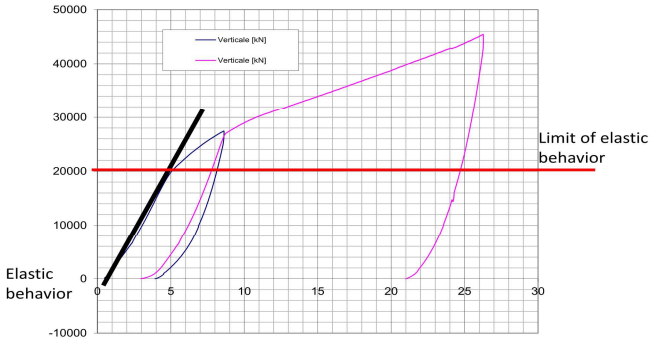

Thus we have $Fcrit = 20000KN$ for the ½ scaled isolator.

$$\tau_{crit} = \frac{2Fh}{\pi R^3} = \frac{2 * (20 * 10^6) * 5}{\pi * 245^3} = 4{,}33Mpa$$

d) Definition of f:

We have seen before that choosing f equal to zero ensures safety standards. The choices of the points where the first damage will be sought limit the value of the compression reached. This definition of f will allow us find the first damage for small compression, the choice of points ensures that the criterion will not be too powerful.

e) Final domain:

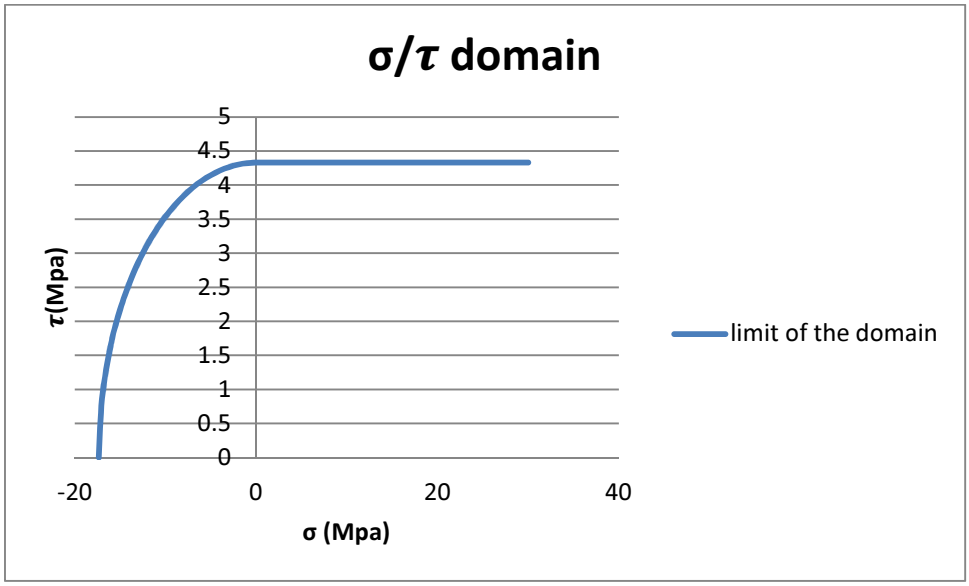

C. Analytical H/V domain:

1. Stresses in function of the considered failure point:

It has been assumed that the first damage is reached when for the first time the $\sigma/\boldsymbol{\tau}$ criterion is exceeded.

The thickness of a rubber layer will be noted h while the height of the isolator will be named H.

For the shear stresses and the normal stress due to the vertical load the single layer solution will be use. The normal stress due to the horizontal load is taken from the solution on the whole isolator and will decide at what height the failure occurs. The principal of superposition will be used.

We've seen that we consider that the failure will occur on the border of the isolator (x=R) and on the top of one of the rubber layer because it's were the total shear stresses are the higher. This mean that for the three stresses calculated on the single layer solution z will be taken equal to h. Therefore we will have the following expressions:

$$\tau_{zx\_vertical} = \frac{2Fhr}{\pi R^4}\cos\left(\frac{\pi z}{h}\right) = \frac{2Fh}{\pi R^3}$$

$$\sigma_{z\_vertical} = -\frac{2F}{\pi R^2}\left(\frac{R^2 - r^2}{R^2}\right) = 0$$

$$\tau_{xz\_horizontal} = 2k(c_{10} + c_{01}) + 4k^3(c_{20} + c_{11} + c_{02})$$

We also showed that the failure will occur first in the traction zone if it exits. Therefore to calculate the normal stress due to the horizontal load we chose the height were the traction is the higher on the border (x=R), this occurs for z=H/2 and the stress has the following form:

$$\sigma_{z\_horizontal} = kcos\left(\frac{\pi x}{R} + \frac{k\pi}{3R}\left(z - \frac{H}{2}\right)\right) = k$$

2. Resultants once the failure is identified:

Using the repartition of the stresses that were obtained in the analytical model we determined the resultants in function of the stresses:

$$H = \tau_{xz\_horizontal}\, \pi R^2$$

$$V = \tau_{zx\_vertical} \frac{\pi R^3}{h}$$

3. Procedure to calculate the domain:

Every vertical load is associated to a different a horizontal load that leads to first damage. We can seek the first damage varying the horizontal or the vertical load. For simplicity reason the domain has been calculated by browsing the possible horizontal loads. The value that in fact has been browsed is the relative displacement k as it is directly linked to the horizontal load. k starts with the value 0 (pure vertical load) and is increased until when the associated vertical load that leads to the crisis is 0 (pure horizontal load).

A value of k is chosen; from this value the stresses due to the horizontal load can be calculated. The normal stress due to the vertical load is considered zero thus the criterion depends only on the value of the total shear stress. Therefore this total shear stress can be calculated to impose the crisis through the following expression:

$$\tau_{total} = \tau_{crisis} \sqrt{1 - \left(\frac{\sigma_{z_{horizontal}} + 0}{\sigma_{crisis}}\right)^2}$$

The shear stress due to the vertical load is calculated using the superposition principal:

$$\tau_{zx\_vertical} = \tau_{total} - \tau_{xz\_horizontal}$$

The resultant are then calculated in function of the stresses with the previous formula.

This procedure is presented in the following figure:

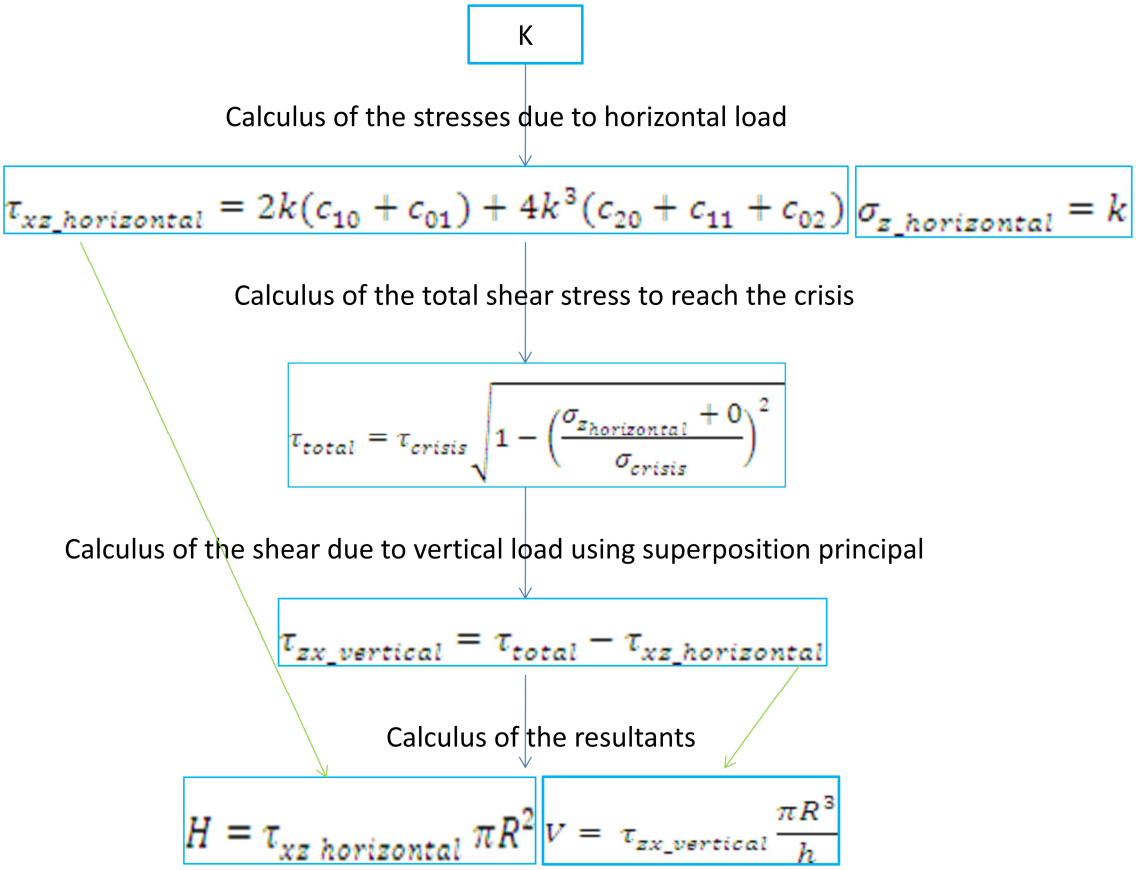

4. Result:

The maximum horizontal relative displacement that is reached when V=0KN is 2,5. The following graphic is obtained:

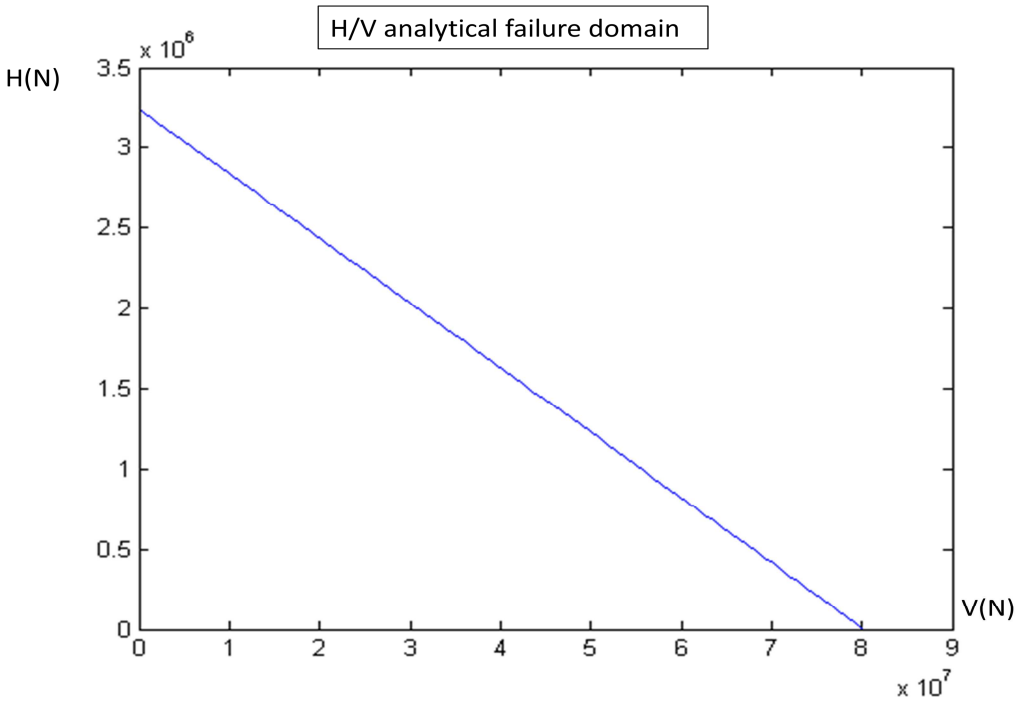

D. Numerical domain:

1. Calculus of the post-processed shear stress:

For reason of numerical cost the numerical domain was calculated with an isolator which parameter e is 4. We have shown before that the optimal parameter will be around 16. In further developments if the total number of elements allowed is increased (license problems) the analysis should be effectuated with the optimal number e.

It has been demonstrated that the only quantity that was sensitive to the mesh refinement was $\tau_{zx\_vertical}$ and that the refined solution was assimilable to the analytical solution. In the post processing of the data the value of $\tau_{zx_vertical}$will be replaced by the analytical value. The following formula will be used; the superposition principal is used in the procedure and has been proven before:

$$\tau_{xztotal\_postprocessing} = \tau_{xztotal\_ansys} - \tau_{xzvertical\_ansys} + \tau_{xzvertical\_analytical}$$

2. Procedure:

The domain has been plotted with 12 points. The model is first loaded with an assigned vertical load and then deformed until the 400% of the isolator height. The data are then post processed and the displacement where the failure criterion is exceeded (when the following formula is more than one) for the first time in one node is sought.

The calculated criterion is

$$\left(\frac{\tau_{xztotal_{postprocessing}}}{\tau_{xzcrit}}\right)^2 + \left(\frac{\sigma_z}{\sigma_{zcrit}}\right)^2 = 1$$

3. Results:

The following domain has been calculated:

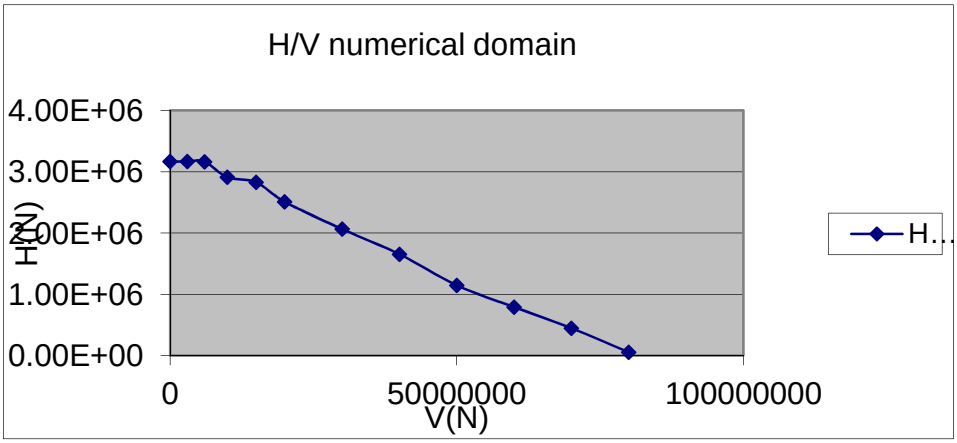

The maximum displacement is 2,4.

E. Comparison of the domains:

The previous results are compared:

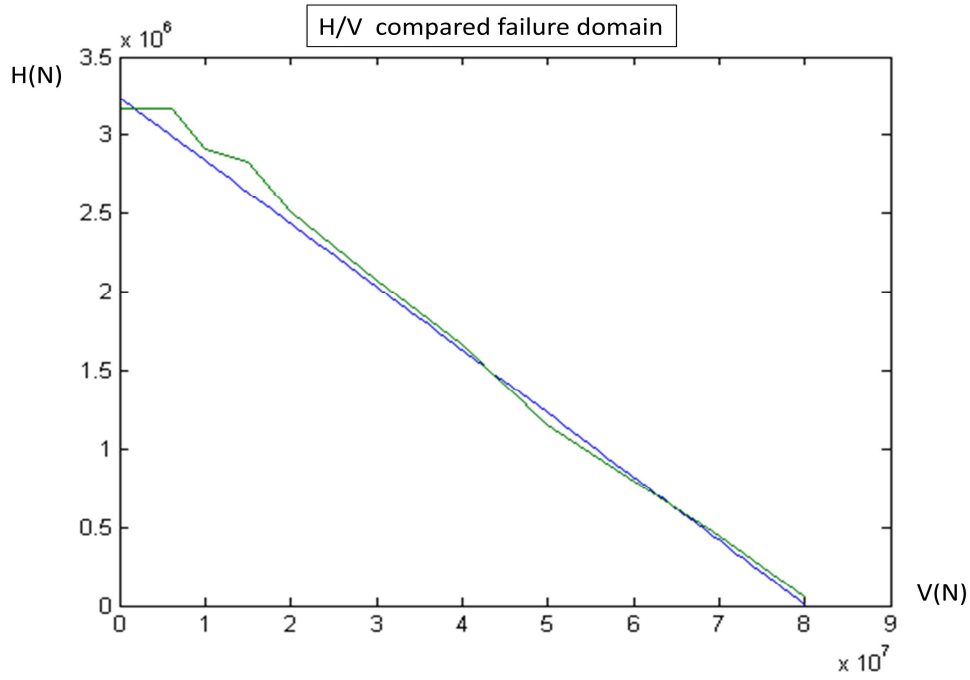

The domains are really closed. The differences that appear can partly be explained by the fact that in the numerical method the horizontal displacement is imposed step by step. If the crisis occurs between two steps it generates imprecision.

The normal numerical and analytical normal stresses are a bite different at the border; the domain is not influenced by these differences. In fact we can conclude that the model is much more sensible to the shear stress than to the normal stress (along z).

F. Compressibility effects on the domain:

From the compressibility study we know that the main stress sensitive to compression is the shear stress due to the vertical load. To take into account this effect the shear stress will be modified in both analytical and numerical cases to match with the stress of a single compressive layer with e 16.

First we have to redefine the new σ/$\boldsymbol{\tau}$ domain. We can have to approach to redefine it: we want to define a more accurate domain of our isolator taking into account the compressibility and working with the data we have or we want to study the effect of taking into account or not the compressibility when defining a domain with standard data.

In the first case the fixed data is the vertical load that leads the system to crisis, in the second one the standard data that define the domain for an isolator is the limit shear stress. Both cases will be studied.

In both cases we have $\tau_{comp} = \alpha\tau_{incomp}$

1. The domain of the studied isolator with compressibility:

The data we have for our isolator is the maximum vertical load (pure compression) 80000KN. I.e. the critical shear stress have to coincide with a vertical load of 80000KN in all the cases. For every new material (K=2450 and K=4550) we define a new critical shear stress with the following expression:

$$\tau_{crit_{comp}} = \tau_{crit_{incomp}} \frac{\tau_{e16\_comp}}{\tau_{e16\_incomp}} = \alpha\tau_{crit_{incomp}}$$

The new critical stress is bigger than the incompressible one.

The vertical load calculated to plot the numerical domain takes the following form:

$$V = \frac{\tau_{xzvertcomp}\pi R^3}{2h\alpha}$$

The results are presented comparing the two compressible solutions and the incompressible one:

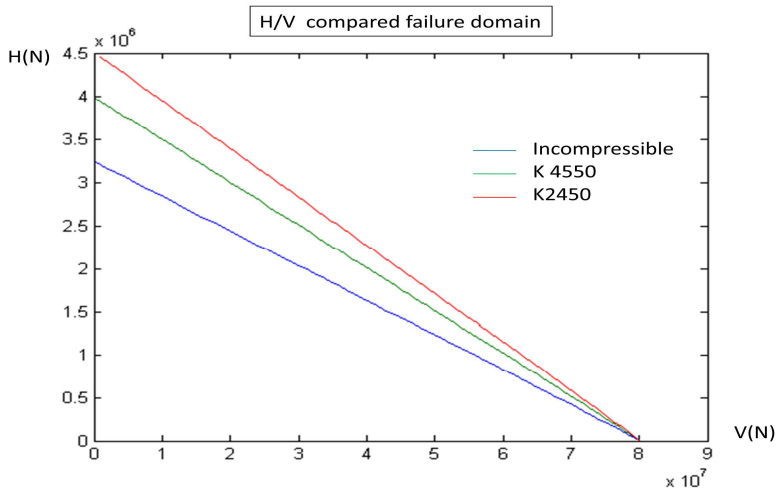

2. Influence on the compressibility in a standard procedure:

In a standard procedure the quantity that should be defined is the limit shear stress because it characterizes the material local behavior and it's therefore independent of the geometry.

In this case $\tau_{crit}$is a data and the vertical load takes the following form:

$$V = \frac{\tau_{xzvertcomp}\pi R^3}{2h}$$

The result is the following:

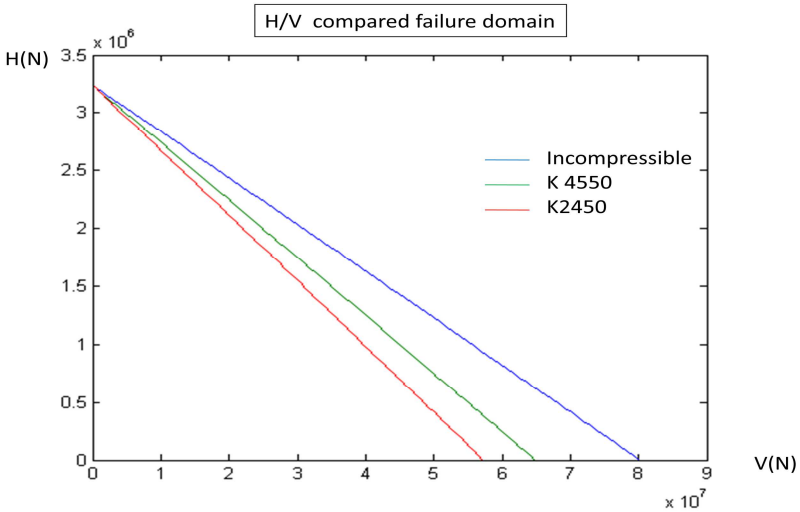

Conclusion:

The work is framed in the research activities performed at the Department of Structural Engineering of Politecnico di Milano on seismic isolation of NPPs buildings, with specific attention to IRIS™ project (International Reactor Innovative and Secure™), a medium size pressurized water reactor, under development by an international consortium. In particular, the study presented here, related to HDRB isolation systems, is mainly functional to accomplish step 4 (first damage limit state domain) of the procedure described by F. Perotti et al. [1], proposing an innovative approach for the evaluation of seismic fragility for isolated buildings:

- step 1: performance of laboratory tests on high damping rubber and HDRB isolating devices;

- step 2: development of a reliable and efficient isolator FE model, taking into account all significant sources of mechanical and geometrical nonlinearities; the model, after having been validated against experimental data, will be used to simulate additional and more complex numerical tests;

- step 3: FE model calibration based on laboratory tests;

- step 4: statement of limit state conditions for the isolator, expressing the interaction between horizontal and vertical load at first damage and failure;

- step 5: isolation system fragility analyses.

A recent study published by Politecnico di Milano ([9]) dealt with step 2 and 3, whose results were assumed as basis for the present study. In the paper, a refined FE model of a single thin rubber layer was developed to investigate the capabilities of multiple hyperelastic material models (Ogden, Polynomial and Mooney-Rivlin), in terms of numerical convergence and goodness of fit, tuned against laboratory tests on rubber specimens. Subsequently, a complete FE HDRB model, closely representing the alternate rubber and steel layers, was set using the best material models, derived from single rubber layer analyses. This preliminary work permitted to develop a robust FE model for a HDRB and to identify Polynomial hyperelasticity as the most promising constitutive law for actual tasks.

In the present work, the geometry and mechanical properties of the HDRB studied in ([9]) were changed to account for the most recent design of IRIS™ isolated layout. It has to be noted that general conclusions about FE modelling and constitutive law assessments obtained from previous isolator matched current results.

The first part of the work analyzed the stress state in the HDRB. A refined FE model of a single rubber layer was set to perform preliminary evaluation on mesh sensitivity and potential sources of numerical instabilities. It has been shown that the number of FEs adopted in thickness plays a crucial role in tangential stresses due to vertical load, whose magnitude affects the limit state domain significantly. Furthermore, global behavior of the FE model was compared with experimental results performed at FIP laboratories on 1:2 scaled isolators. It resulted in optimum agreement for what concerns horizontal stiffness, while vertical stiffness is highly affected by exact estimation of rubber compressibility.

The paper Corradi et al. [10] proposed an analytical formulation for stresses in a single rubber layer (Corradi-Guiducci solution), subjected to vertical and horizontal loading

separately, based on approximate solution in large displacement, for different hyperelastic constitutive laws. The Corradi-Guiducci solution was found to be accurate in predicting all but one stress state also in the HDRB, since rubber layers behave almost as single individual rubber layers in series. The present work extended and applied this solution to the complete isolator, allowing predicting also vertical normal stresses in the complete isolator, which is significantly different than the Corradi-Guiducci solution for a single rubber layer. The proposed Modified corradi-guiducci analytical formulation was compared to numerical solutions and was considered to be accurate in predicting the stress field in the HDRB devices subjected to vertical load and horizontal displacement, at least in regions was first damage is more likely to occur.

Extensive numerical tests were performed to verify the possibility to decouple horizontal and vertical actions. The error due to superimposing the effects of each load condition was found small enough to confirm that analytical solutions developed separately for horizontal and vertical loads could be superimposed, without significant error in first damage domain assessment.

Rubber compounds may suffer damage and fail for delamination, tensile rupture, tearing, fatigue and cavitation. Delamination damage condition is accounted in present study by a Mohr – Coulomb limit state domain, tuned against mechanical properties provided by the manufacturer, in terms of rubber tensile strength and maximum tangential stress due to maximum vertical load. In the second part of the work, the HDRB first damage domain was addressed by means of the FE model and analytical solution. Both approaches led to convergent bi-dimensional first damage domains, expressed in terms of maximum horizontal load for a given vertical load. The domain represents the combination of forces that provoke the very first damage at a single location inside the HDRB, whose bearing capacity and stiffness properties are still unchanged.

The study has been mostly developed for full incompressible rubber, although significant results were obtained in case of nearly incompressible rubber. It has been shown that tangential stresses due to vertical load and vertical normal stresses due to horizontal displacement are highly affected by actual rubber bulk modulus, whose precise evaluation becomes mandatory and has to be provided by the manufacturer. In particular, for current geometry and mechanical properties, the tangential stresses due to vertical load was found to strongly affect the domain, since they significantly increase as compressibility is slightly increased. Thus, considering rubber full incompressible may lead to not conservative safety assessments. The manufacturer should obligatorily provide the tangential limit stress of the rubber and the compound at interface.

Bibliography:

Chapter one:

[1] G. Bianchi, M. Domaneschi, D.C. Mantegazza and F. Perotti, "A procedure for the computation of seismic fragility of NPP buildings with isolation base", ANS PSA 2011 International Topical Meeting on Probabilistic Safety Assessment and Analysis Wilmington, NC, March 13-17, 2011, American Nuclear Society, LaGrange Park, IL (2011)

[2] A. Der Kiureghian, "Non-ergodicity and PEER's framework formula", Earth. Eng. Struct. Dyn., 34, pp. 1643-1652 (2005)

[3] Henri P. Gavin , Siu Chung Yau, "High Order Limit State Functions in the Response Surface Method for Structural Reliability Analysis", Preprint submitted to Elsevier Science (2007)

[4] FIP Industriale, ENEA Centro Ricerche Bologna, "Rapporto di prova FIP Industriale VP 59/10" (2010)

[5] Alessandro Martelli, Massimo Forni, "La protezione degli impianti nucleari dai terremoti e dai maremoti", Il giornale dell'Ingegnere (15 april 2011)

Chapter two:

[6] Corradi Dell'Acqua Leone, "Meccanica delle strutture, Volume1: il comportamento dei mezzi continui", McGraw Hill, Milano (1992)

[7] Holzapfel Gerhard A., "Nonlinear solid mechanics: a continuum approach for engineering", John Wiley & Sons, Chichester (2000)

[8] ANSYS® Structural, ANSYS® Inc., "Theory Reference, Chapter 4: Structures with material nonlinearities"

Chapter three:

[7] MSC software corporation, "Non linear finite element analysis of elastomers, technical paper" (2000)

[8] MSC software corporation, "Experimental elastomer analysis" (2005)

[9] G. Bianchi, L. Corradi dell'Acqua, M. Domaneschi, D. C. Mantegazza, F. Perotti," High Damping Rubber Bearing (HDRB) isolating devices for nuclear power plants: FE modelling and damage characterization", SEWC (2011)

[10] Corradi dell'Acqua L., Domaneschi M., Guiducci C., "Assessing the reliability of seismic base isolators for innovative power plant proposals", 20th International Conference on Structural Mechanics in Reactor Technology (SMiRT20), Espoo Finland, August 9-14, 2009.

[11] Imbimbo M., De Luca A., "F. E. stress analysis of rubber bearings under axial loads,Computers & Structures" 68, 31-39 (1998)

[12] S.B. Bhoje, P. Chellapandi, S. Chetal, R. Muralikrishna, T. Salvaraj, "Comparison of computer simulated and observed force deformation characteristics of anti-seismic devices and isolated structures" Indira Gandhi Centre for Atomic Research India

[13] M. Forni, A. Martelli, A. Dusi, G. Castellano, “Hyperelastic Models of Steel-Laminated Rubber Bearings for Seismic Isolation of Civil Buildings and Industrial Plants” Abaqus user’s conference in Paris (1995)

Chapter four:

[14] J.R. Xiao and J.W. Gillespie, “A Phenomenological Mohr-Coulomb Failure Criterion for Composite Laminates under Interlaminar Shear and Compression”, Journal of Composite Materials 41, 1295-1311 (2007)

[15] Gillespie, J.W., Gama, B.A., Cichanowski, C.E. and Xiao, J.R.), “Interlaminar Shear Strength of Plain Weave S2-Glass/SC79 Composites Subjected to Out-of-Plane High Strain Rate Compressive Loadings”, Comp. Sci. Tech., 65(11–12): 1891–1908 (2005)

[16] Alan N. Gent, “Engineering with rubber, How to design a rubber components, 2nd edition”, Hanser Publishers Munich, Hanser Garfner Publications Inc Cincinnati (2001)

[17] A. Corigliano, “Damage and fracture mechanics techniques for composite structures”, 3.11 of Encyclopedia of Comprehensive Structural Integrity (CSI), Elsevier (2002)